Naval Ocean Research and Development Activity
April 1989 Report 212

The Polar Ice Prediction System— A Sea Ice Forecasting System

Ruth H. Preller
Ocean Sensing and Prediction Division
Ocean Science Directorate

Pamela G. Posey
Berkeley Research Associates
Springfield, Virginia

Executive Summary

The Polar Ice Prediction System (PIPS), based on the Hibler dynamic/thermodynamic sea ice model, was developed as an upgrade to the existing sea ice products available at the U.S. Navy's Fleet Numerical Oceanography Center (FNOC). It was also designed to provide new sea ice products that could be used as guidance by the Naval Polar Oceanography Center (NPOC). The operational testing of PIPS showed that the ice drift from the model was excessive in magnitude when compared to ice drift from Arctic buoys. As a result, the PIPS forcing was changed from planetary boundary layer model winds to geostrophic winds calculated from forecast surface pressures. Resultant PIPS ice drifts were more accurate than those calculated by the existing operational model—the Thorndike and Colony free-drift model. The operational test also indicated a need to reduce the model time step from 24 to 6 hours. Reducing the time step allowed for better resolution of atmospheric heat fluxes and improved the model's capability to predict ice edge location. PIPS results also showed great improvement when updated by an ice concentration analysis for the Arctic derived by NPOC. This updating technique is now an integral part of the PIPS system and takes place approximately once per week.

As a result of this testing and the associated improvements made to the model, PIPS was declared operational on 1 September 1987. Examples of PIPS output and results from model-data comparisons are presented.

Acknowledgments

The authors would like to acknowledge the expert assistance of Mr. Ken Pollak in the design and implementation of the Polar Ice Prediction System. We would also like to thank Mr. R. Michael Clancy and Mr. Ken Pollak for reviewing this manuscript. Funding for this project came from the U.S. Navy Space and Naval Warfare Systems command through the Air Ocean Prediction program (Program Element 63207N) under Captain J. J. Jensen.

Contents

The Polar Ice Prediction System—A Sea Ice Forecasting System

I. Introduction

Prediction of sea ice characteristics in the polar oceans is of great practical interest, as location of the ice edge, ice thickness and ice concentration impact both naval and commercial operations. In recent years, real-time forecasting of ice motion, ice thickness and ice edge location (concentration) has been emphasized with operational models now running at the Fleet Numerical Oceanography Center (FNOC) and at the National Meteorological Center (NMC).

Early sea ice forecasting models run at FNOC used empirical models of interactions between wind, ice, and ocean. The first such forecast models predicted only ice drift. The Skiles model (Skiles, 1968) defined ice drift based on geostrophic winds and mean ocean currents. The empirical results obtained by Skiles were based on a limited data set relating 15 days of ice drift from four ice stations to mean sea-level pressure fields from the U.S. Weather Bureau and mean annual currents from the U.S. Navy's Hydrographic Office. The Skiles model was replaced by the Thorndike and Colony (1982) model in 1983, a free-drift model. This model is based on a relationship between geostrophic wind, ice and ocean currents determined by a statistical analysis of 5 years of drifting buoy data. Although this model predicts the motion of pack ice fairly well, it does not take into account the important effects of changes in ice thickness, and ice concentration and internal ice stress on ice motion.

In addition, FNOC also uses the Gerson model (Gerson, 1975) to predict ice thickness at a number of specified points in the Arctic. This model uses statistical procedures based on the relationship between degree-day accumulation and the growth and decay of ice to forecast the ice thickness at a particular location.

Over the past 10 years, great strides have been made in designing highly sophisticated sea ice models. The first of these models concentrated on the correct thermodynamic treatment of ice and its interaction with the atmosphere and ocean (Maykut and Untersteiner, 1971; Bryan et al., 1975; Semtner, 1976; Washington et al., 1976; Parkinson and Washington, 1979; and Manabe et al., 1979). Free-drift models, such as the Skiles (1968), the Thorndike and Colony (1982) and the Overland et al. (1984), concentrated on the dynamic interaction of air, ice and water. The theoretical work of Thorndike et al. (1975), Rothrock (1975) and Coon (1974) enabled the development of dynamic/thermodynamic ice models. Thorndike et al. designed an areal ice thickness distribution function. In this model, thin ice is redistributed dynamically into thicker ice categories (ridging) in response to deformation. Thermodynamic effects cause the relative amounts of ice in each category to change. Rothrock provided a means to couple ice thickness to the ice rheology by suggesting that the rate of work done on ice by ridging is related to work done by ice interaction forces. Coon developed the concept of a plastic constitutive law for sea ice. These ideas were combined with the thermodynamic sea ice model of Semtner (1976) to form a dynamic/thermodynamic sea ice model (Hibler, 1979; 1980).

In 1984, the Naval Ocean Research and Development Activity (NORDA) began to test the Hibler ice model as a possible operational forecast model at FNOC. The Hibler model has the advantage of being able to predict not only ice drift, but also ice thickness and ice concentration (ice edge). Full implementation of the Hibler ice model at FNOC was completed in the summer of 1985. The sea ice forecasting system was designated the Polar Ice Prediction System (PIPS). During fall 1985 through fall 1986, an operational test of PIPS was conducted. The test involved comparisons of ice drift from PIPS versus ice drift from the existing operational model (Thorndike and Colony). Both model drifts were also compared to actual drifting buoy data. In addition, ice edge forecasts from PIPS were tested against the ice edge determined by the Naval Polar Oceanography Center (NPOC).

This report provides a brief technical description of this model, presents results of the operational test, and describes the PIPS output.

II. Description of the Model

The Polar Ice Prediction System uses the Hibler dynamic/thermodynamic sea ice model as its basis. The ice model is defined by five major components: a momentum balance, ice rheology, ice thickness distribution, ice strength and an air/ice/ocean heat balance.

The momentum balance used to determine ice drift is given by

$$m \frac{D\vec{u}}{Dt} = m f \hat{k} \times \vec{u} + \vec{\tau}_a + \vec{\tau}_w - mg \, grad \, H + \vec{F},$$

where m is the ice mass per unit area, $\vec{u}$ is the ice velocity, f is the Coriolis parameter, $\vec{\tau}_a$ and $\vec{\tau}_w$ are the air and water stresses, g is the acceleration of gravity, H is the sea surface dynamic height and $\vec{F}$ is the force due to variation in the internal ice stress. Ice is considered to move in a two-dimensional field with forcing applied through simple planetary boundary-layer formulations.

The air and water stresses are defined using constant turning angles

$$\tau_a = \rho_a C_a | \vec{U}_g | (\vec{U}_g \cos \phi + \hat{k} \times \vec{U}_g \sin\phi)$$

$$\tau_w = \rho_w C_w | \vec{U}_w - \vec{u} | [(\vec{U}_w - \vec{u}) \cos\theta + \hat{k} \times (\vec{U}_w - \vec{u}) \sin\theta] \quad ,$$

where $\vec{u}$ is the ice drift velocity, $\vec{U}_g$ is the geostrophic wind, $\vec{U}_w$ is the geostrophic ocean current, C_a and C_w are the air and water drag coefficients, ρ_a and ρ_w are the air and water densities and ϕ and θ are the air and water turning angles. For a more detailed discussion of model dynamics and the spatial finite differencing code, see Hibler (1979).

The ice rheology, a viscous-plastic constitutive law, relates the ice stress to ice deformation and ice strength in the following manner:

$$\sigma_{ij} = 2\eta (\varepsilon_{ij}, P) \varepsilon_{ij} + [\zeta (\varepsilon_{ij}, P) - \eta (\varepsilon_{ij}, P)] \varepsilon_{kk} \delta_{ij} - P\delta_{ij}/2,$$

where σ_{ij} is the two-dimensional stress tensor, ε_{ij} is the strain tensor, $P/2$ is a pressure term, and ζ and η are nonlinear bulk and shear viscosities. Ice flows plastically for normal strain rates and deforms in a linear viscous manner for small strain rates.

The ice thickness distribution takes into account the ice thickness evolution as a result of dynamic and thermodynamic effects. The PIPS model originally used a two-level approach (Hibler, 1979). This approach designates that ice is broken up into two categories, thick and thin, and that the division between the two is 0.5 m. The compactness, A, is defined as the area within a grid cell covered by thick ice, while $(1 - A)$ is the area covered by thin ice. This treatment resulted in an average ice thickness over the Arctic, which was too thin when compared to observations (Preller et al., 1986). To correct for this bias and to include the strong dependence of ice growth rates on thickness, a seven-level ice thickness calculation used by Walsh et al. (1985) was added to the PIPS model in March 1988. This method divides the "thick" ice into seven categories and allows ice to grow/decay in each category. The seven levels are equally spaced between 0 and twice heff, where heff is the effective ice thickness (Hibler, 1979) or mean ice thickness over the entire grid cell. For periods of ice growth, snow cover is also divided into a seven-level linear distribution of snow depths equally spaced between 0 and two times the grid cell mean. When melting occurs, snow is assumed to be uniformly distributed over the ice covered portion of the grid cell. Snowfall rates are based on monthly mean climatological values (Maykut and Untersteiner, 1969; Parkinson and Washington, 1979). This improved treatment of thick ice resulted in an average increase of ice thickness of 50 cm over the PIPS domain.

The equations for thickness and compactness are

$$\frac{\partial h}{\partial t} = - \frac{\partial (uh)}{\partial x} - \frac{\partial (vh)}{\partial y} + S_h + diffusion$$

$$\frac{\partial A}{\partial t} = - \frac{\partial (uA)}{\partial x} - \frac{\partial (vA)}{\partial y} + S_A + diffusion \, ,$$

where S_h and S_A are thermodynamic terms defined by

$$S_h = f\left(\frac{h}{A}\right) A + (1 - A) f(0)$$

$$S_A = \begin{cases} \frac{f(0)}{h_o} (1 - A) & \text{if } f(0) > 0 \\ 0 & \text{if } f(0) < 0 \end{cases}$$

$$+ \begin{cases} 0 & \text{if } S_h > 0 \\ \left(\frac{A}{2h}\right) S_h & \text{if } S_h < 0 \quad , \end{cases}$$

with $f(h)$ as the growth rate of ice of thickness h (heff) and h_o a fixed demarcation between thick and thin ice. In all model simulations, $h_o = 0.5$ m. In the seven-level ice thickness calculation, heff is the averaged seven-level sum of ice thickness, including the calculated snow and ice thickness changes. The term S_h is the net growth or melt of ice. S_A is the change in compactness due to the growth or decay of ice.

Ice strength is treated as a function of the ice thickness distribution and compactness given by the equation

$$P = P^* h \exp [- C (1 - A)] \, ,$$

where P^* and C are fixed empirical constants, h is the ice thickness, and A is the compactness. This relationship shows the strength of ice to be strongly dependent on the amount of thin ice $[(1 - A)]$. It also allows the ice to strengthen as it becomes thicker.

The thermodynamic portion of the code determines growth and decay rates of ice based on a heat budget balance between the atmosphere, ice and ocean including the effects of heat absorbed by leads via lateral mixing. Similar to Semtner's (1976) formulation, heat is transferred through the ice by assuming a linear temperature profile along with a constant ice conductivity. When open water is losing heat to the atmosphere, the heat budget growth rates are taken to be vertical growth rates. When open water absorbs heat, the heat mixes underneath the flows to reduce the vertical growth rate. Any remaining heat can either cause lateral melting or raise the temperature of the mixed layer. In the presence of an ice cover, the mixed-layer temperature is always set equal to freezing. Thus, excess heat absorbed by leads is used for lateral melting until the ice disappears. During growth conditions, ice is not allowed to form until the mixed layer reaches the freezing temperature of seawater.

In the two-level version of the model, following Bryan et al. (1975) and Manabe et al. (1979), the effects of snow cover are treated such that the ice surface albedo is that of snow (0.75) when the calculated surface temperature is below freezing and is that of snow-free ice (0.616) when the surface temperature is at the melting point. Thus, the upward heat flow, I_h, through ice of thickness h is

$$I_h = (K/h)(T_w - T_o),$$

where K is the ice conductivity, T_w is the water temperature, and T_o is the surface temperature of the ice.

In the two-level case, snow is parameterized only through the surface albedos while the new seven-level formulism uses the accumulated rates from Maykut and Untersteiner (1969) and Parkinson and Washington (1979). The thermal conductivity in the seven-level case is a single value based on a weighted sum of snow and ice conductivities

$$\frac{K_s K_I}{(K_s Sn_{l,l} + K_I h_{l,l})},$$

where $h_{l,l}$ is the ice thickness at that level, $Sn_{l,l}$ is the snow depth at the same level, K_s is the snow conductivity, and K_I is the ice conductivity. The prescribed surface albedos used by Walsh et al. are 0.80 for snow and 0.65 for ice.

The surface heat budget, after Parkinson and Washington (1979) and Manabe et al. (1979), is given by

$$\begin{aligned}(1-\alpha)F_s + F_l + D_l|\vec{U}_g|(T_a - T_o) \\ + D_s|\vec{U}_g|[q_a(T_a) - q_s(T_o)] \\ D_s T_o^4 + (K/H)(T_w - T_o) = 0,\end{aligned}$$

where α is the surface albedo, T_o is the surface temperature of ice, T_a is the air temperature, T_w is the water temperature, $\vec{U}_g$ is the geostrophic wind, q_s is the specific humidity of the ice surface, F_s is the incoming short wave radiation, F_l is the incoming long wave radiation, D_l is the bulk sensible heat transfer coefficient, D_s is the bulk latent heat transfer coefficient (water or ice) and D_s is the Stephan-Boltzman constant times the surface emissivity. This surface heat budget defines a surface temperature for the ice which balances the heat budget. This temperature then determines the conduction of heat through the ice and the growth rate. If the derived temperature is above freezing, it is set back to the freezing point. Surface and bottom ablation rates are then determined by the imbalances in the surface heat budget and by conduction of heat into the mixed layer. Heat transfer from the deep, warmer, ocean water can either be treated as a constant or as a variable heat flux into the mixed layer. For a detailed discussion of the thermodynamic portion of the model, see Hibler (1980). A detailed listing of the values associated with the parameters used by this model may be found in Table 1 of Preller (1985).

Model Grid: The operational PIPS grid was designed as a subsection of the FNOC Northern Hemisphere polar stereographic grid. The model grid covers a region including the central Arctic, Barents Sea and the northern half of the Greenland-Norwegian Seas. An averaged mapping factor is used to approximate equal spacing for the FNOC polar stereographic grid in the region of the PIPS domain. The ice model grid is defined as an equally spaced, 127-km grid subset of the FNOC northern hemisphere polar stereographic grid. The resultant ice model dimensions are 47 · 25 (Fig. 1). The operational PIPS model timestep is 6 hours.

All boundaries of the model are solid except for the southern boundary in the Greenland-Norwegian Seas. This region contains two rows of "outflow" grid cells. Ice can be transferred into these grid cells only by advection and once there, flows out of the basin.

III. Forcing

Both atmospheric and oceanic forcing are necessary to drive the ice model. Atmospheric forcing is obtained from the Navy Operational Global Atmospheric Prediction System (NOGAPS) (Rosmond, 1981). This global atmospheric model provides surface pressure fields, which are used to determine geostrophic winds. In addition to surface pressure, the NOGAPS model also provides surface vapor pressure (used in conjunction with surface pressure to determine the specific humidity at the ice surface), surface air temperature, incoming solar radiation (short wave), sensible heat

flux, and total heat flux. The last three fields are used to determine long wave radiation.

Oceanic forcing exists in terms of monthly mean geostrophic ocean currents and deep-ocean heat fluxes. These ocean currents and heat fluxes were derived from the Hibler/ Bryan (1984; 1987) coupled ice-ocean model (Fig. 2). The effects of the variability of ocean currents on ice drift has been shown to be important over long time scales (Thorndike and Colony, 1982). On the time scale of a forecast (5 days), the variability of the ocean currents has a much smaller effect on the ice drift than the variability of the wind stress fields. For this reason, monthly mean ocean currents can be used with some degree of confidence.

Including monthly mean deep oceanic heat fluxes has resulted in a tremendous improvement in the model's capability to predict edge location in the marginal ice zone. Hibler and Bryan (1984; 1987) have shown that this oceanic heat flux can melt large amounts of ice in the marginal ice zone (Fig. 3). Similar results were seen in our testing of the Hibler model coupled to the atmospheric and oceanic forcing described above (Preller, 1985). Figure 4a shows contours of ice thickness for a case with constant oceanic heat flux of 2 $W\text{-}m^2$ (a value normally used in the central Arctic) used over the entire model basin. Figure 4b shows results of a case identical to that shown in Fig. 4a, except that the monthly mean heat fluxes have been used. Including the monthly varying heat flux results in a dramatic improvement in ice edge location.

Ideally, one would prefer to have an ocean model, coupled to the ice model, which can predict the variability of the ocean on the same time and space scales as the ice. To date, however, three-dimensional, coupled, ice-ocean models are still in the development stage.

IV. Initial Conditions

The PIPS model can make use of three different methods of initialization. Each day the model makes a 120-hour forecast. A file that consists of the model's 24-hour forecast of ice thickness, concentration, ice drift, surface ice temperature, and heat absorbed by the open ocean is saved. The model uses this 24-hour forecast as its restart field the next day. If the restart field from the previous day does not exist, the model searches back as far as 1 week. If restart fields are not available, then model climatology is used to restart the model. The model climatology contains monthly mean fields derived from 3 years of model integration driven by 1986 NOGAPS forcing each year. At the end of the 3-year integration, the model has reached a cyclic steady state. These "steady state" solutions form the model climatology.

Once per week (usually Friday), in addition to the restart field, the model is also given a new field of gridded ice concentration. This concentration field is a digitized version of the NPOC weekly ice concentration analysis. The weekly NPOC analysis (Fig. 5) is a subjective analysis derived from all available remotely sensed data (AVHRR, Visible, Passive Microwave) and all available observations (ship, plane, etc.) (NPOC, 1986). This field is hand digitized once per week by NPOC and is transferred to FNOC. The digitized data is then placed on the model grid and read into the model as an update or an initialization field.

The PIPS model assimilates this data in the following manner. A model restart field is read in (either a 24-hour forecast or climatology). PIPS then checks to see if an NPOC analysis field is available. If the analysis field is older than 4 days or has been used within the past 4 days, then an "update" is not made. Otherwise, if the NPOC analysis is available, the model replaces its entire forecasted ice concentration field with the NPOC analysis. Two additional fields are then updated: the ice thickness and the heat stored by the ocean. The new concentration field is compared to the model-derived concentration field. If no ice exists where it did exist before the update, then the ice thickness is set equal to zero and a small amount of heat is added to the open-ocean mixed layer. If concentration has been added to a previous open-ocean region, then the ice thickness is updated in the following manner

If $0.15 < A < 0.5$ and $H < 0.5$, then $H = 0.5$

or

If $A > 0.5$ and $H < 0.5$, then $H = 1.0$

and heat is removed from the mixed layer.

V. Run Schedule and Output Fields

The PIPS model is run once per day, producing a 120-hour forecast on the 00Z GMT watch. The length of the PIPS forecast is limited by the length of the NOGAPS forecast (120 hours).

Model results, output at 6-hour intervals, are saved during each forecast period and are available for distribution near 0600 GMT. Products are sent to NPOC via the Naval Environmental Display System (NEDS) graphics. The PIPS model produces six different output fields in conjunction with each day's run. Included with these six PIPS fields is an associated product used for comparison with the PIPS results; surface pressure fields from the NOGAPS model with Planetary Boundary Layer Northern Hemisphere (PBLNH) model winds overlaid. The following fields are chosen from the model's forecast results to be sent to NPOC as NEDS graphic products:

1. Ice Drift (cumulative)	Tau 24, 48, 72, 96, 120
2. Ice Thickness	Tau 0, 120
3. Ice Concentration	Tau 0, 120
4. Divergence convergence	Tau 48, 96, 120
5. 120-hour ice thickness difference	
6. 120-hour ice concentration difference	
7. Surface pressure with PBLNH winds	Tau 0, 120

Tau indicates the forecasted time from the initialization of the day's run (i.e., Tau 24 is a 24-hour forecast). These output fields have been specifically chosen to provide guidance products to NPOC. The 120-hour difference field for ice thickness and concentration were specifically designed to assist in making a weekly forecast of ice concentration and ice edge location.

The PIPS model provides nine new sea ice products when compared to previous operational models (Gerson and Thorndike and Colony). In addition, PIPS provides all sea ice information on a higher resolution grid than its predecessors. The only present disadvantage of the PIPS model is its coverage. The PIPS domain size is limited by the existing ocean currents and heat fluxes. Thus it is limited to a basin size similar to that used by Hibler and Bryan. This problem is being addressed in basic research and development programs at NORDA, as well as other laboratories and universities where coupled ice-ocean models are being designed.

The PIPS job stream functions on two mainframes. The NOGAPS model is run on the (4-Pipe) CYBER 205. The output from NOGAPS, the ocean currents and heat fluxes, the model climatology and the model restart fields are all stored on the CYBER 205. The NPOC analysis of ice concentration is stored on a CYBER 860. The ice model is run on the CYBER 205 and generates output fields, which are then transferred to and plotted on the CYBER 860. A 120-hour forecast requires approximately 50 seconds of cpu time on the CYBER 205 and approximately 60 seconds of cpu time on the CYBER 860.

VI. Verification Techniques

A. User Evaluation of PIPS Output Products

The user evaluation of PIPS was performed for NPOC by Walter B. Tucker III of CRREL and William D. Hibler III of Dartmouth College. The model evaluation was done in two phases. In Phase I, which extended from 15 November 1985 to 15 March 1986, the model was initialized strictly from its own generated restart field or from a model-derived climatology. During Phase II, which extended from 15 June 1986 until 15 October 1986, the model was updated approximately once per week using a digitized ice analysis prepared by NPOC. In both cases the primary output products evaluated were ice drift, ice concentration, and ice edge. The Phase I evaluation was performed in a qualitative manner due to the lack of initialization update data available during that period. The Phase II evaluation was performed in a much more quantitative manner (Tucker and Hibler, 1987a). The findings of Tucker and Hibler were reviewed by NPOC, and a summary of this review was forwarded to FNOC at the end of the test period. The findings of the evaluation, plus additional quantitative evaluation studies performed by NORDA, will be discussed in the following sections.

B. Statistical Comparisons with Buoy Observations

The drifting buoys in the Arctic have been monitored by the Arctic Ocean Buoy Program at the University of Washington's Polar Science Center (PSC) (Colony and Munoz, 1985) since 1979. PSC reviews essentially raw data from the Service Argos system in particular, position, atmospheric pressure and temperature. These buoy positions, which are recorded approximately hourly, are presumed accurate to within a few hundred meters. For purposes of model verfication, a daily average buoy position from PSC is used to determine ice drift. The positions are given as latitude-longitude locations determined out to three decimal places. At present, ice drift is the single model output, which can be evaluated in a highly quantitative manner.

Comparisons made in these evaluations included comparing not only PIPS ice drift to buoy drift, but also comparing the drift from the existing operational model (the Thorndike and Colony model) to the buoys and to PIPS. For PIPS to be declared an operational model, its ice drift should be at least as good as or better than that of the existing operational model.

In performing these comparisons it must be noted that the buoy drift represents the drift of a particular ice flow, which may not move in the same manner as the ice that surrounds it. PIPS ice drift, however, represents an average ice movement over a 127-km^2 area.

As a result of the evaluation performed by Tucker and Hibler, NORDA also performed an evaluation using model ice drift derived using 1983 NOGAPS forcing (a NORDA standard test data set) versus the 1983 PSC buoy data. For this evaluation a number of statistical values were calculated, such as the mean and standard deviation of each data set and the mean error and root-mean-square error between data sets, as well as an index of agreement (after Willmott, 1981; 1985).

C. Comparison of Model Ice Concentration to Ice Concentration from NPOC

Aside from ice drift, a somewhat quantitative comparison can also be made of model ice concentration to the ice concentration derived from a subjective weekly analysis available at the Navy/National Oceanic and Atmospheric Adminstration Joint Ice Center (JIC) (NPOC, 1986). The PIPS concentration fields and ice edge were quantitatively compared to the NPOC analysis and evaluated by Tucker and Hibler (1987b). Included in this paper are quantitative comparisons of the most recent PIPS model ice concentration and ice edge information to the NPOC dat .

VII. Operational Test Results

A. Phase I Results

The Phase I evaluation (Tucker and Hibler, 1986) took place during winter conditions in the Arctic. For this reason, qualitative evaluations of ice edge were performed only in the Greenland Sea and the Barents Sea because the Chukchi Sea was ice covered. Comparison showed that the model ice edge was located farther south than indicated by the NPOC analysis. Week-to-week displacements of the edge, however, were generally in the right direction. The conclusion drawn was that without any initialization data, the model predicted too much ice in the winter in the marginal ice zone. This excessive amount of ice is probably due to errors both in the atmospheric forcing and in the crude temporal and spatial variability of the oceanic forcing.

When model ice drift was qualitatively compared to buoy drift, they agreed reasonably well in direction but were biased fast. Model drift agreed better with buoy drift in the Beaufort Sea than in the central Arctic.

During the Phase I evaluation, the FNOC CYBER 205 was down for approximately 1 week. As a result, the PIPS model was initialized from the model-derived climatology. This event revealed two points about the PIPS system. First, it could be successfully restarted from climatology in such an emergency situation and, second, with no other means of initialization it took the model approximately 2 weeks to return to a state similar to that before the restart.

B. Phase II Results

1. Comparison with Buoy Observations

The most significant change to the PIPS for the Phase II evaluation was the addition of a weekly update/initialization of the system by the digitized ice analysis from NPOC. Whenever the entire analysis is available at FNOC, it is incorporated into the model and replaces the model-derived field. The digitized NPOC field undergoes quality control before being used by the model. When the field reaches FNOC, a NEDS graphic product is created. This graphic is reviewed by both NPOC and FNOC. If the product is not satisfactory, then it not used. If it is satisfactory, the field undergoes additional machine quality control before it is accepted. The date of the initialization usually lags the analysis date by 3 days (analysis Tuesday, update Friday).

During this evaluation, a more regional statistical study of ice drift, ice concentration, and ice edge was made. Eighteen buoys were available during the total Phase II period, with approximately 12 available at any one time. None of these buoys was located in the eastern Arctic, so the comparison was related strictly to the central and western Arctic.

Cumulative vector plots were calculated for three individual periods of approximately 37 days each. The cumulative vector plots were calculated by summing the x and y components of 10 chosen forecast days during the 37-day period (usually as a Wednesday and a Saturday forecast). Buoy locations were interpolated to the model grid and ice drift calculated from the location change. Tucker and Hibler showed that the PIPS model drifts were excessive in most cases when compared to the buoy drift. They also found that the error in direction was highly variable, depending upon the location of the particular buoy observed and the time of the year (August directional error was the largest of the three summer months). Tucker and Hibler also compared PIPS cumulative drift to the drift derived from the operational free-drift model (Fig. 6). This figure showed that the magnitude of the drift from the free-drift model was substantially less than that of PIPS and often was in better agreement with the observed buoy drift.

Tucker and Hibler (1987b) calculated statistics for forecast buoy drifts over 24-hour intervals accumulated over the 10-day forecast period (Table 1, Tucker and Hibler, 1987b). The x and y component errors (Δx and Δy) and the mean error vector magnitude ratio ($Ve/Vobs$) show the PIPS drift to be too large in magnitude, with $Ve/Vobs$ ratios varying from 100 to 200%. High correlation coefficients (Rx, Ry) indicated that a linear relationship existed between observed and predicted drifts, which implies that the correction to this magnitude problem may be a simple linear correction. Similar statistics performed for each buoy show that model ice drift predictions are best in the Beaufort Sea and are worst along the Alaskan coast. Near Alaska the proximity to the land/sea boundary and the coarse resolution of the model may result in poorly predicted ice drifts. Ice drift error close to the pole, although better than that at the Alaskan coast, seems highly variable.

As a result of the findings from the Tucker-Hibler evaluation of PIPS, an intense statistical study of available wind forcing at FNOC and resultant model-derived ice drift was made by NORDA. For PIPS to successfully pass its evaluation, it must be able to predict ice drift at least as well as or better than the free-drift model. As shown in Figure 6, this was not the case. One would suspect that a model with more complete physics and a detailed ice rheology should show an improved prediction capability. Why did it result in less accurate forecasts of ice drift?

The free-drift model uses geostrophic winds calculated from NOGAPS surface pressure fields. PIPS used the FNOC marine boundary layer winds produced by the PBLNH system (Mihok and Kaitala, 1976), which relates analyzed and forecasted synoptic scale variables predicted by NOGAPS to the small-scale variables that describe the turbulent surface layer. The PBLNH computes vertical profiles of winds as a function of the Monin-Obukov length scale. The winds input into PIPS are calculated at 19.5-m heights (a standard level used for FNOC operational products).

When comparing these two ice drift fields, which are predominantly wind driven, one would hope the wind stress fields are also comparable. Figure 8 shows the eight-day average difference in May of stress from PIPS calculated using the equation

$$\tau_{PBLNH} = \rho_a C_{ap} \vec{v} \vec{v} ; \qquad C_{ap} = 2.7 \times 10^{-3}$$

minus the surface wind stress calculated from geostrophic winds using

$$\tau_{geo} = \rho_a C_{ag} \vec{U}_g (U_g \cos\phi + k \times U_g \sin\phi) ;$$

$$C_{ag} = 1.2 \times 10^{-3} \quad \phi = 23^\circ .$$

This result shows that the PBLNH wind stress is larger than the geostrophic wind stress by more than 1 dyne/cm^2 in a number of regions. The only place where the PBLNH stress is less is in a small region about the pole. The PBLNH stresses are originally calculated on a spherical grid and then interpolated to polar stereographic. This results in a singular point at the pole. Thus winds near the pole are often erroneous. If the difference between these wind stress magnitudes was due strictly to the drag coefficient, then one would expect a constant difference over the domain. Figure 7 shows that this is not the case.

As a result, identical test cases of the PIPS model were run using 1983 NOGAPS forcing with only one difference. In the first case, the PBLNH marine winds were used. In the second case, geostrophic winds calculated from NOGAPS surface pressure were used. Statistical comparisons were performed on these two data sets, compared to buoy data and also to ice drift from the free-drift model.

For this series of tests, 22 buoys were available, although not all were available over the entire year. Figure 8 shows the monthly mean 24-hour forecast magnitude of the ice drift averaged over all available buoys. Note that except for February, the PIPS model driven by the PBLNH winds gave the largest drifts. When driven by geostrophic winds, resultant PIPS ice drift was generally smaller and in better agreement, but was not as good as the ice drift from the Thorndike and Colony model. To improve the comparison of the PIPS model with the buoy drift, the drag coefficients were reduced until the best agreement with buoy data was reached. Best agreement was reached when the drag coefficient for the PBLNH was reduced to 1×10^{-3} (approximately a factor of 3) and when the drag coefficient for geostrophic winds was reduced to 0.8×10^{-3} (a factor of 1.4). A value of 1×10^{-3} is an extremely small drag coefficient for surface winds. Therefore, geostrophic winds, using the 0.8×10^{-3} drag coefficient, was chosen as the more realistic approximation. Use of the geostrophic winds also reduced error in the region near the pole where the PBLNH winds contained a singular point. Figure 9 shows the comparison of mean PIPS drift driven by geostrophic winds with $C_D = 0.8 \times 10^{-3}$ to the free-drift model and to buoy observations. Note that the PIPS model is now better than the free-drift model for 8 out of the 12 months.

Figure 10 shows the monthly averaged 24-hour forecasted RMS error between PIPS driven by geostrophic winds and buoy data and the free-drift model and buoy data. Note that from January through May and from July through August, the RMS errors are almost equal to each other and are less than 15 cm/sec. From September through December the average RMS error rises in both cases, but PIPS does substantially better in October and November. PIPS is also dramatically better than free drift in June. This increase in RMS error for free drift takes place during the months of seasonal transition in the Arctic, and could indicate that free drift was not a good assumption for ice during this period of changing ice conditions.

Figure 11 shows the monthly averaged 24-hour forecast index of agreement between PIPS and the buoys and free drift and the buoys. The index of agreement reflects the degree to which the observed value (buoy) is accurately estimated by the predicted value (PIPS or free drift). It is not a formal measure of correlation, but is a measurement of the degree to which a model's predictions are error free. The index of agreement is expressed as

$$d = 1 - \frac{\sum_{i=1}^{N} (P_i - O_i)^2}{\sum_{i=1}^{N} (|P_i| + |O_i|)^2} ,$$

where

O = observed value
P = predicted value

and

$$P' = P - \bar{O}$$
$$O' = O - \bar{O}$$

where

$\bar{O}$ = observed mean
$\bar{P}$ = predicted mean.

A value of 1.0 (100%) indicates perfect agreement between predicted and observed values (Willmott, 1981). The trends of the index of agreement follow the trends in the RMS error quite closely. During all months except April and August, the PIPS model has a higher index of agreement. The index of agreement for free drift is also particularly poor during the seasonal transition periods as indicated by the RMS.

2. Ice Concentration—Ice Edge Comparisons

PIPS concentration and ice edge location forecasts were evaluated by comparing them to the digitized ice analysis from NPOC. Although the model update takes place approximately 3 days after the analysis, for these comparisons, the date of the update will be used as the analysis date.

Tucker and Hibler performed a series of comparisons and some statistical analyses of the PIPS forecasts during the summer period of July-October 1986. They found a number of trends appearing in the data. First, the PIPS model forecast lower concentrations in the central Arctic then the NPOC analysis. Part of this difference is because the NPOC analysis often assigns a 100% concentration to the central Arctic where observations are scarce. They also found that the model ice edge often retreated too quickly in the western Arctic, resulting in an excessive amount of open water in the Chukchi Sea. Agreement was far better in the eastern Arctic. Although the ice edge occasionally advanced too quickly, good agreement was observed, even in situations when the model had not been updated for 3 weeks.

C. NORDA's Evaluation

After the model's operational evaluation, a change was made to the model's time step, reducing it from 24 hours to 6 hours. This reduction would resolve the daily variability of the solar radiation and atmospheric heat fluxes and thus improve the ice edge forecast. In addition, the model forcing was changed to use geostrophic winds as discussed in the previous section. After these changes were implemented, a second evaluation of the model was performed by NORDA. Evaluation of the PIPS model is an ongoing effort at NORDA.

1. Ice Drift vs. Buoy Drift

Starting on 17 June 1987, NORDA began to obtain buoy fixes from the Service ARGOS system on a daily basis (Fig. 12). A statistical study similar to that presented in section VI B was conducted. Statistics were performed on consecutive, approximately 2-week-long, data sets over the period of 1 year. Table 1 shows the mean, Table 2 shows the RMS error, and Table 3 shows the index of agreement for the ice drift magnitudes from this year-long test. We have included in these tables, the upper and lower bound values associated with the 95% confidence interval. The confidence limits are calculated using a nonparametric approach from Efron (1981a, 1981b) and Efron and Gong (1983), called the "bootstrap." The bootstrap makes no a priori assumptions about the probability density function being analyzed, but creates an empirical distribution function by resampling a set of N independent observations (Willmott et al., 1985).

This test case shows that PIPS results are better than free drift in the mean; however, they have similar RMS errors and PIPS has a slightly better index of agreement. From the RMS error values, it appears that both models have similar "statistical" accuracy. The index of agreement shows that both models are close to and often significantly greater than 0.5 in all but the summer months. This statistic indicates that both models are significant error-reducing descriptions of ice drift in all but the summer months. Although the index of agreement implies that neither model is an outstanding predictor of ice drift magnitude in the summer, PIPS compares more closely with the observations in the mean than does free drift during this time.

2. Ice Concentration — Ice Edge

A new comparison of model ice edge and ice concentration vs. NPOC analysis was performed on model results derived after the change to a 6-hour time step. Similar to Tucker and Hibler, we drew ice concentration along seven designated lines across the PIPS domain (Fig. 13). Representative winter and summer data sets were chosen. A 24-hour model forecast was compared to an NPOC analysis for that same day. Note that for the winter data (April), all comparisons were made 7 days after an update (Figs. 14a and 14b). Results show excellent agreement between the model ice edge and the NPOC analysis in the western Arctic. In the eastern Arctic, the agreement is fairly good; however, the model can predict too much or slightly too little ice at the edge. Agreement is very good in the central Arctic in winter.

Figures 15a and 15b show summer results along the same seven lines. Results are from cases where the model was updated either 7 or 21 days prior to the comparison. Note that in September, the peak of Arctic summer, the model results show that the ice edge

retreated too far north in the western Arctic. However, there is good agreement at the ice edge in the western Arctic by October.

Figures 16a and 16b show the mean concentration error for the entire line dependent upon the number of days since update for winter and summer. Comparison to a similar figure done by Tucker and Hibler for 1986 PIPS results (Tucker and Hibler, 1987b) shows that the error in 1987 has been reduced at the 7- and 21-day intervals. In both cases, large error is seen along line 23, a location near the Soviet coast. Poor PIPS results in this region are probably due to the proximity of the model boundary and lack of resolution of the coast at this boundary. As observed by Tucker and Hibler, the mean concentration error for a 7-day update is less than that for a longer update (21 days).

Figures 17a and 17b show mean ice edge error (model-data) in summer for each line averaged over the two 7-day and two 21-day update cases. Note that in both cases all but two of the values fall within ±63 km or one-half a grid distance, the expected error of the model. Results from the cases updated 7 days prior to the run have slightly smaller error than cases updated 21 days prior to the run. The magnitude of the error for the eastern and western Arctic is

Table 1. Mean drift (m/sec).

	BUOY CONFIDENCE LIMITS (95%)			PIPS CONFIDENCE LIMITS (95%)			FREE DRIFT CONFIDENCE LIMITS (95%)		
1987	VALUE	LOWER	UPPER	VALUE	LOWER	UPPER	VALUE	LOWER	UPPER
617	.1065	.0688	.1635	.0928	.0733	.1166	.0538	.0415	.0608
724	.0690	.0340	.1026	.0854	.0694	.1103	.0561	.0463	.0691
809	.0754	.0370	.1477	.0739	.0580	.0896	.0447	.0346	.0537
825	.0780	.0321	.1371	.0770	.0553	.1048	.0513	.0373	.0660
909	.1015	.0643	.1443	.0912	.0680	.1152	.0560	.0418	.0702
1008	.1050	.0298	.2020	.0908	.0623	.1158	.0650	.0495	.0797
1114	.0778	.0372	.1210	.1184	.0836	.1552	.0832	.0580	.0960
1219	.0555	.0373	.0778	.1055	.0790	.1328	.0713	.0560	.0878
1988									
105	.0788	.0532	.1144	.0964	.0754	.1214	.0656	.0520	.0808
124	.0985	.0572	.1523	.0898	.0695	.1198	.0692	.0548	.0835
210	.0722	.0415	.0943	.0767	.0568	.1022	.0626	.0500	.0793
229	.0776	.0549	.1043	.0849	.0626	.1094	.0616	.0477	.0765
322	.0915	.0630	.1248	.0972	.0725	.1253	.0610	.0485	.0985
412	.1043	.0683	.1580	.1078	.0783	.1445	.0763	.0568	.0985
430	.0954	.0664	.1270	.0932	.0730	.1162	.0646	.0550	.0816
526	.0625	.0442	.0845	.0629	.0461	.0839	.0484	.0370	.0615

Table 2. RMS error (m/sec).

	PIPS CONFIDENCE LIMITS (95%)			FREE DRIFT CONFIDENCE LIMITS (95%)		
	VALUE	LOWER	UPPER	VALUE	LOWER	UPPER
617	.0692	.0570	.1432	.1155	.0530	.1633
724	.0723	.0484	.0956	.0689	.0399	.0894
809	.0879	.0531	.1220	.0884	.0451	.1287
825	.1168	.0596	.1746	.1101	.0504	.1667
909	.0907	.0647	.1175	.0982	.0605	.1330
1008	.1862	.1018	.2740	.1788	.0800	.2730
1114	.0982	.0670	.1296	.0898	.0544	.1180
1219	.0790	.0528	.1043	.0528	.0375	.0678
105	.0694	.0470	.0932	.0606	.0328	.0910
124	.1220	.0603	.1677	.1158	.0435	.1667
210	.0717	.0402	.1035	.0708	.0390	.1060
229	.0736	.0454	.0994	.0691	.052	.0896
322	.0652	.0403	.0878	.0647	.0457	.0860
412	.1110	.0535	.1615	.1055	.0490	.1543
430	.0630	.0360	.0910	.064	.0374	.0904
526	.0473	.0275	.0667	.0445	.0267	.0621

Table 3. Index of agreement (%).

	PIPS CONFIDENCE LIMITS (95%)			FREE DRIFT CONFIDENCE LIMITS (95%)		
	VALUE	LOWER	UPPER	VALUE	LOWER	UPPER
617	.4765	.2400	.6755	.4152	.2627	.5597
724	.5726	.3030	.7690	.4890	.2750	.6739
809	.2941	.1300	.5830	.3051	.0973	.4899
825	.2187	.0449	.5067	.2673	.0510	.5098
909	.5390	.2578	.7115	.5008	.3215	.6445
1008	.2642	.0850	.5070	.2825	.0933	.5007
1114	.6296	.3180	.8016	.5160	.2790	.6876
1219	.4730	.2048	.7023	.4740	.2012	.6985
105	.5506	.3038	.7356	.5458	.2908	.7966
124	.3815	.1788	.5383	.3760	.1927	.5703
210	.6182	.3365	.8372	.5285	.2322	.7370
229	.4644	.2610	.7137	.5780	.3367	.6051
322	.6553	.3842	.8452	.6192	.3812	.7945
412	.4103	.2313	.6883	.4155	.2758	.6330
430	.5646	.2990	.7836	.5574	.2770	.7352
526	.6005	.3675	.7904	.5546	.3343	.7494

approximately the same for the case 7 days after update, but 21 days after updating, error noticeably increases in the western Arctic, indicating that the ice edge is farther north than observed.

Winter results (Fig. 18) are all from cases 7 days after update. All values from these results fall within one-fourth grid distance error, showing very good agreement between the model and the data.

3. Ice Thickness

A comparison of forecast ice thickness to observed ice thickness during the period of the evaluation was not possible, since observations of ice thickness are both temporally and spatially scarce. However, PIPS ice thickness has been compared qualitatively to seasonal and yearly averaged ice thickness derived from submarine data (LeSchack et al., 1971; Garrett, 1985). These comparisons (Preller et al., 1986) showed that the PIPS model developed a realistic ice cover with thickest ice developing along the Canadian Archipelago, thinning towards the pole, and continuing to decrease from the pole toward the Soviet coast (Fig. 4b).

A comparison of PIPS ice thickness versus submarine data (Garrett, 1985) was also done basin by basin. Garrett examined data from the years 1960, 1962, 1967, 1971, 1973, and 1975-1982. From this data he calculated a mean ice thickness for eight different regions in the Arctic. It should be noted that data was not available in every basin for each season or even each year. The PIPS model was run with the same oceanic forcing but with several different years of NOGAPS forcing (1983, 1986, 1987). Unfortunately, NOGAPS atmospheric forcing was not available until 1983, so there are no results that compare directly to the years with submarine data; however, certain trends are seen from year to year. Figures 19a and 19b show comparisons of model results from 1986 and 1987 to the submarine data. Our 1987 PIPS results were often updated by the NPOC analysis, while 1986 results used no update data. Similar trends exist in both years with two main differences. The 1986 results generally have thicker ice in all basins except for the Greenland Sea. This increase in ice thickness is due to the implementation of the Walsh et al. (1985) seven-level ice thickness calculation in the 1986 test case. Poor agreement in the Greenland Sea in both cases is due to PIPS' tendency to develop very thin ice in the Greenland Sea in the summer and fall. Results in 1987 are slightly better than 1986 because the model was updated with the NPOC analysis. The update corrected the ice thickness near the ice edge, thus adding more ice to the Greenland Sea. In general, the agreement between model and data is fairly good. One would expect agreement between data and the model to improve as more observational data becomes available (more years and seasons for each basin) and more model runs (more years) are made to create a better average.

The NORDA evaluation showed a definite improvement in the PIPS model over the Tucker and Hibler evaluation in both the ice drift and ice concentration assessments. This improvement was due to use of more accurate wind forcing (geostrophic winds) and higher accuracy in the atmospheric fluxes due to a 6-hour versus 24-hour time step.

VIII. Example PIPS Output

PIPS presently outputs 14 fields as NEDS graphic products. The following figures are PIPS results from 14 November 1987. In general, the fall represents a period of southward-advancing ice in all parts of the Arctic.

Ice drift is represented as "cumulative" ice drift and is output at Tau 24, 48, 72, 96, 120. Cumulative drift vectors are created by adding resultant ice drift vectors "head to tail" at every time step. Figure 20a is the 24-hour forecasted cumulative ice drift from the 00Z 14 November run. Figure 20b is the NOGAPS surface pressure field with the PBLNH winds overlaid at Tau 0. Figure 20c is the geostrophic wind field calculated from NOGAPS surface pressures (from the NORDA 24-hour forecast run). Note that the pattern developed by the ice drift closely follows the wind except for the turning of the drift slightly to the right of the winds. Figure 21a is the cumulative ice drift over the 120-hour forecast, and Figure 21b is the 120-hour forecast NOGAPS surface pressure. The drift pattern established in the 24-hour forecast is still observed in the 120-hour forecast. The only change is when the center of the anticyclonic circulation in the East Siberian sea shifts toward the northeast due to the movement of the pressure centers during the 5-day forecast.

Figure 22a shows the ice concentration at Tau 0 and Figure 22b shows the 120-hour forecasted ice concentration. The concentration in the central Arctic is approximately 100%. Gradients of ice concentration become tight at the ice edge in the Greenland, Barents, and Beaufort Seas. The dark black line in Figure 22a is a coarse-resolution, ice edge message sent weekly to FNOC by NPOC. The most recent update of the ice model was on 30 October 1987, 15 days prior to this run. These results show an increase in ice concentration and an extension of the ice edge southward in the Kara, Beaufort, and Chukchi Seas, as well as in the area west of Spitzbergen. These results agree with observations from this period, except in the region west of Spitzbergen. The PIPS model often predicts too much ice west of Spitzbergen because of the coarse resolution used by the Hibler-Bryan model (160 km), which does not resolve the West Spitzbergen Current or the heat carried by that current.

Figures 23a and 23b are the ice thickness fields at Tau 0 and at the Tau 120 forecast. The ice thickness contours show maximum thickness along the Canadian Archipelago (4 m), thinning toward the pole. At Tau 0, a small amount of open water still exists in the model along the Alaskan coast and in the Beaufort Sea, but by Tau 120 ice appears to have reached most of the coast.

Figures 24a and 24b are the 5-day forecast change in ice concentration and ice thickness. Changes in both thickness and concentration are almost all positive, indicating the growth of ice and advance of the ice edge. Maximum changes in ice thickness are 30 cm in the Beaufort and Kara Seas, while the maximum change in ice concentration is 40% in the Beaufort Sea and 50% in the Kara Sea. These changes in ice thickness and concentration are confirmed by the 18 November 1987 NPOC analysis, the closest analysis to the date of the 120-hour forecast.

IX. Summary

The Polar Ice Prediction System (PIPS) is a dynamic/thermodynamic sea ice model used at FNOC to forecast ice drift, ice thickness, and ice concentration. The PIPS model covers the central Arctic, as well as the Barents Sea, and the northern half of the Greenland and Norwegian Seas. Predecessors to the PIPS model at FNOC were the Gerson Model and the Thorndike and Colony free-drift model. PIPS predicts not only ice drift at a higher resolution than the existing free-drift model, but also the effects of growth and decay of ice. As a result, PIPS produces nine additional products over its' predecessors.

An operational test of PIPS was performed in two phases by Tucker and Hibler (1986; 1987). Phase I extended from 15 November 1985 to 15 March 1986 and consisted of a qualitative analysis of the model's results. Phase II extended from 15 June 1986 until 15 October 1986. During Phase II, the model was updated approximately every week by an ice concentration analysis from NPOC. Tucker and Hibler concluded that the magnitude of the ice drift from PIPS was too large. They also concluded that, although some error did exist in matching the predicted model ice edge to the NPOC ice edge, trends of ice growth and decay predicted by the model were accurate. They also found that the model's forecasting ability improved with the frequency of updates.

In response to these findings, NORDA and FNOC improved the PIPS model by changing the wind forcing from the PBLNH winds to geostrophic winds derived from NOGAPS surface pressures and by reducing the time step from 24 hours to 6 hours. A statistical study of the model driven by geostrophic winds showed that the upgraded PIPS model now forecasted ice drift at least as well as or better than the free-drift model. A quantitative study similar to that done by Tucker and Hibler showed that these changes also improved the model's ability to predict ice concentration and ice edge location.

Based on these improved results, the PIPS model was declared operational on 1 September 1987. PIPS is constantly monitored on a daily basis by both NORDA and FNOC. Plans for the existing PIPS model include the development of blending schemes to blend all available data into the "best possible" update field for the model. In addition, FNOC is presently running its first high-resolution regional model, the Barents Sea model, for initial testing. The Barents Sea model uses the ice thickness from PIPS as a boundary condition for its northern, open boundaries. Future ice forecasting models expected to become operational at FNOC are additional regional models, such as a Greenland Sea model, and coupled ice-ocean models.

X. References

Bryan, K., S. Manabe, and R. Pacanowski (1975). A global ocean-atmosphere climate model, Part II- The oceanic circulation. *Journal of Physical Oceanography* 5:30-46.

Colony, R. and E. Munoz (1985). *Arctic Ocean Buoy Program Data Report, 1 January 1983 - 31 December 1983.* Polar Science Center, Applied Physics Laboratory, University of Washington, Seattle, Washington.

Coon, M. D., S. Maykut, R. Pritchard, D. Rothrock, and A. Thorndike (1974). Modeling the pack ice as an elastic-plastic material. *AIDJEX Bulletin* 24:1-105.

Efron, B. (1981a). Nonparametric estimates of standard error: The jackknife, the bootstrap and other methods. *Biometrika* 68:589-599.

Efron, B. (1981b). Nonparametric standard errors and confidence intervals. *Canadian Journal of Statistics* 9:139-172.

Efron, B. and G. Gong (1983). A leisurely look at the bootstrap, the jackknife and cross-validation. *American Statistics* 37:36-48.

Garrett, R. P. (1985). *Temporal and Spatial Distributions of Arctic Sea Ice Thickness and Pressure Ridge Statistics.* Naval Postgraduate School, Monterey, California, Report 68-85-009.

Gerson, D. J. (1975). *A Numerical Ice Forecasting System.* Naval Oceanographic Office, Stennis Space Center, Mississippi, Report N00 RP 8.

Hibler, W. D. (1979). A dynamic thermodynamic sea ice model. *Journal of Physical Oceanography* 9:815-846.

Hibler, W. D. (1980). Modeling a variable thickness sea ice cover. *Monthly Weather Review* 108:1944-1973.

Hibler, W. D. and K. Bryan (1984). Ocean circulation: Its effects on seasonal sea-ice simulations. *Science* 224:489-491.

Hibler, W. D. and K. Bryan (1987). A diagnostic ice-ocean model. *Journal of Physical Oceanography* 17:987-1015.

Le Schack, L. A., W. Hibler, and F. Morse (1971). Automatic processing of Arctic pack ice obtained by means of submarine sonar and other remote sensing techniques. *Propagation Limitations in Remote Sensing,* J. B. Lomax (Ed.), *AGARD Conf. Proc.* 90:5-19.

Manabe, S., K. Bryan, and M. Spelman (1979). A global ocean-atmosphere climate model with seasonal variation for future studies of climate sensitivity. *Dynamics of Atmosphere and the Ocean* 3:393-426.

Maykut, G. A. and N. Untersteiner (1969). *Numerical Prediction of the Thermodynamic Response of Arctic Ice to Environmental Changes.* The Rand Corporation, Santa Monica, California, RM-6093-PR.

Maykut, G. A. and N. Untersteiner (1971). Some results from a time-dependent thermodynamic model of sea ice. *Journal of Geophysical Research* 76:1550-1575.

Mihok, W. F. and J. Kaitala (1976). U.S. Navy Fleet Numerical Weather Central operational five-level global fourth-order primitive-equation model. *Monthly Weather Review* 12:1527-1550.

Naval Polar Oceanography Center (1986). *Eastern-Western Arctic Sea Ice Analysis 1986.* Washington, DC.

Overland, J. E., H. Mofjeld, and C. Pease (1984). Wind-driven ice drift in a shallow sea. *Journal of Geophysical Research* 89:6525-6531.

Parkinson, C. L. and W. Washington (1979). A large-scale numerical model of sea ice. *Journal of Geophysical Research* 84:311-337.

Preller, R. H. (1985). *The NORDA/FNOC Polar Ice Prediction System (PIPS) — Arctic: A Technical Description.* Naval Ocean Research and Development Activity, Stennis Space Center, Mississippi, NORDA Technical Report 108.

Preller, R. H., P. Posey, K. Pollak, and R. Clancy (1986). Forecasting ice thickness and concentration in the Arctic using a numerical model. *Proceedings of Second Workshop on Ice Penetration Technology,* U.S. Army Cold Regions Research and Engineering Laboratory, Hanover, New Hampshire.

Rosmond, T. E. (1981). NOGAPS: Navy Operational Global Atmospheric Prediction System. Preprint Volume, Fifth Conference on Numerical Weather Prediction, Monterey, California Published by the *American Meteorological Society,* Boston, Massachusetts, 74-79.

Rothrock, D. A. (1975). The energetics of the plastic deformation of pack ice by ridging. *Journal of Geophysical Research* 80:4514-4519.

Semtner, A. J., Jr. (1976). A model for the thermodynamic growth of sea ice in numerical investigations of climate. *Journal of Physical Oceanography* 6:379-389.

Skiles, F. L. (1968). *Empirical Wind Drift of Sea Ice.* Arctic Drifting Stations, the Arctic Institute of North America.

Thorndike, A. S. and R. Colony (1982). Sea ice motion in response to geostrophic winds. *Journal of Geophysical Research* 87:5845-5892.

Thorndike, A. S., D. Rothrock, G. Maykut, and R. Colony (1975). The thickness distribution of sea ice. *Journal of Geophysical Research* 80:4501-4513.

Tucker, W. B., III and W. Hibler (1986). *An Evaluation of the Polar Ice Prediction System.* U.S. Army Cold Regions Research and Engineering Laboratory, Hanover, New Hampshire.

Tucker, W. M., III and W. Hibler (1987a). An evaluation of an operational ice forecasting model during summer. *Proceedings of POAC,* Fairbanks, Alaska.

Tucker, W. B., III and W. Hibler (1987b). *An Evaluation of the Polar Ice Prediction System—Phase II.* U.S. Army Cold Regions Research and Engineering Laboratory, Hanover, New Hampshire.

Washington, W. M., A. Semtner, C. Parkinson, and L. Morrison (1976). On the development of a seasonal change sea ice model. *Journal of Physical Oceanography* 6:679-685.

Walsh, J. E., W. Hibler, and B. Ross (1985). Numerical simulation of northern hemisphere sea ice variability, 1951-1980. *Journal of Geophysical Research* 90:4847-4865.

Willmott, C. J. (1981). On the validation of models. *Physical Geography* 2:184-194.

Willmott, C. J., S. Ackleson, R. Davis, J. Feddema, K. Klink, D. Legates, J. O'Donnell, and C. Rowe (1985). Statistics for the evaluation and comparison of models. *Journal of Geophysical Resear h* 90:8995-9005.

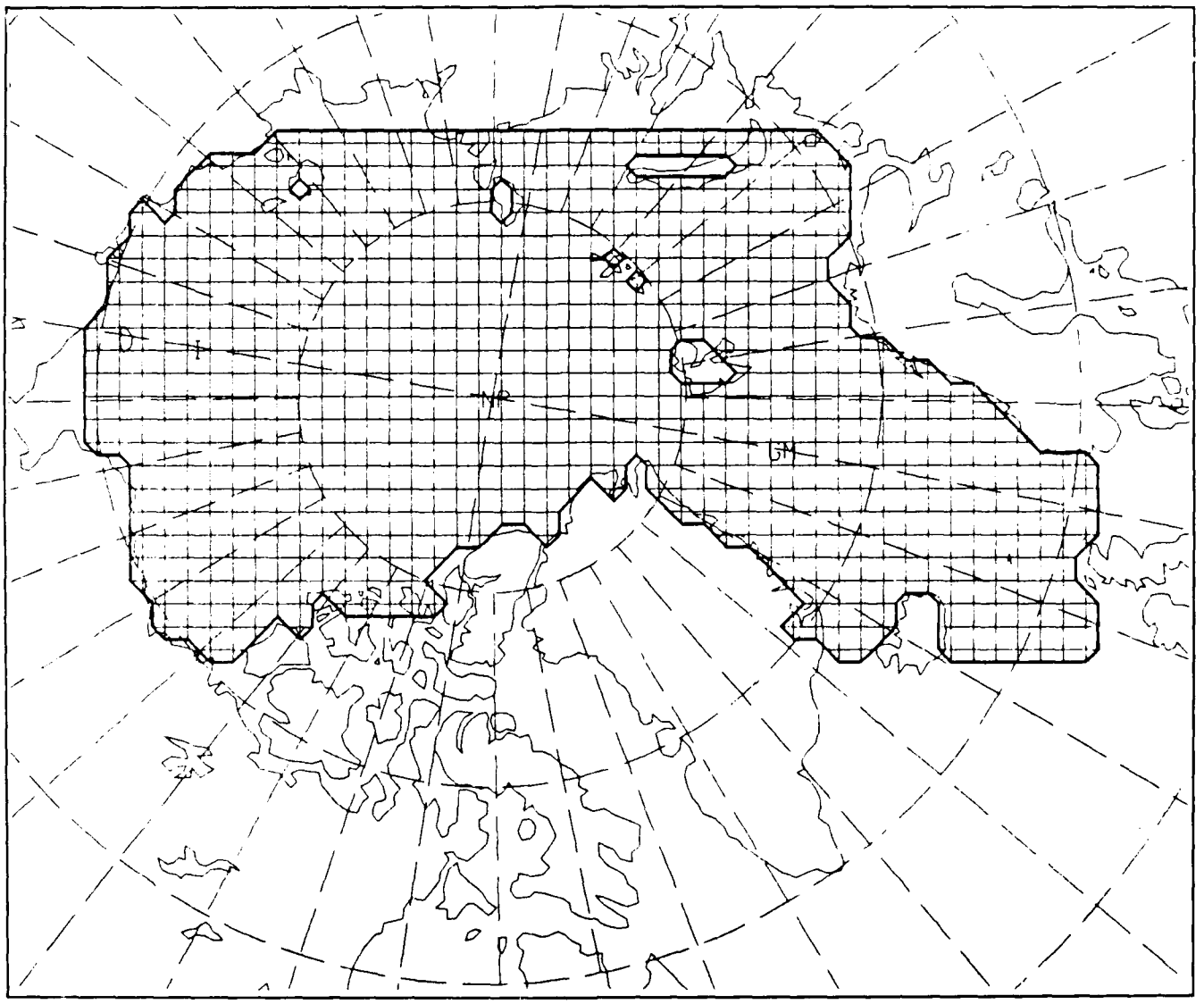

Figure 1. The PIPS model domain with the 127-km resolution grid overlaid.

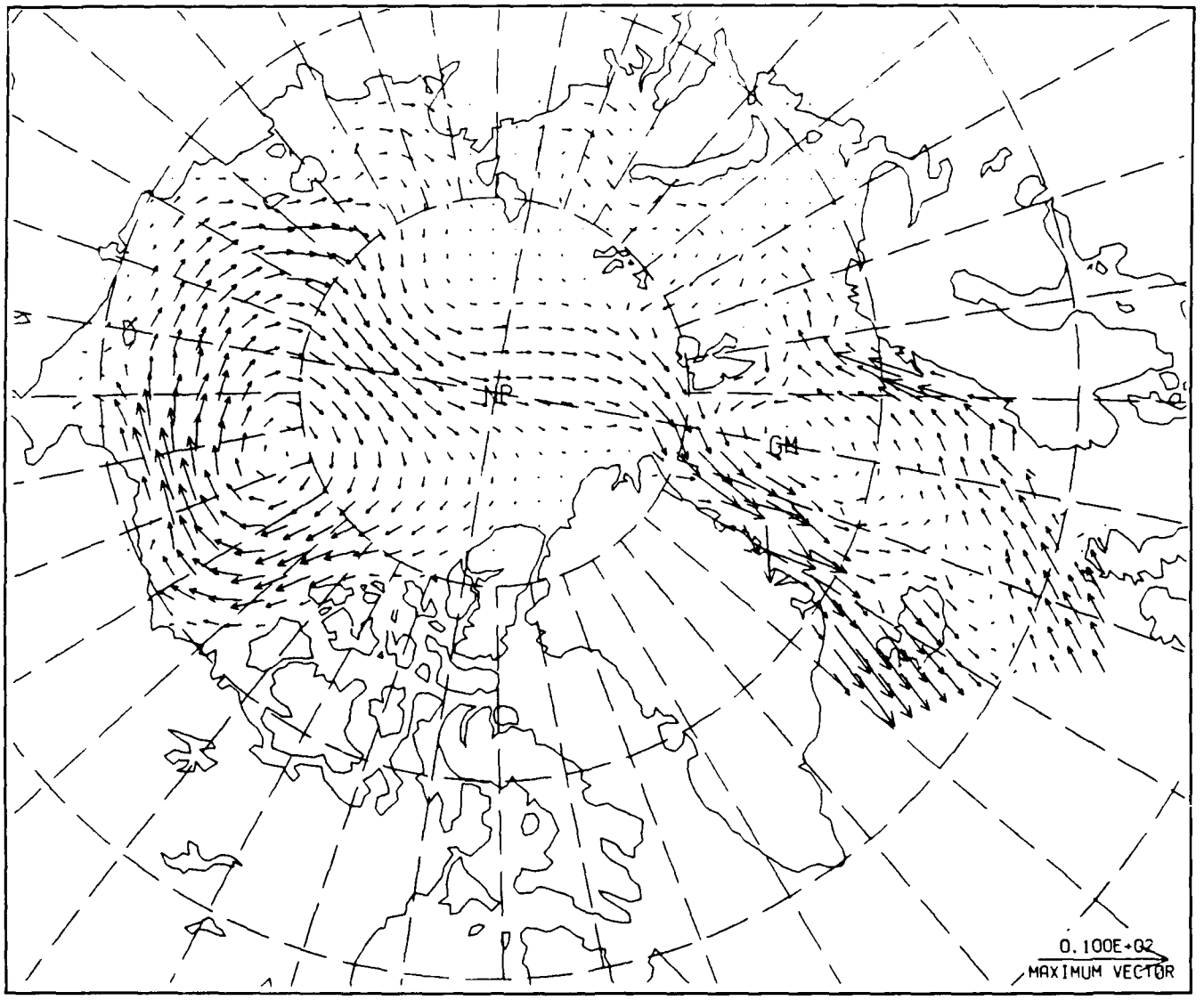

Figure 2. Annual averaged Hibler-Bryan ocean currents. Maximum vector is 0.1 m/sec.

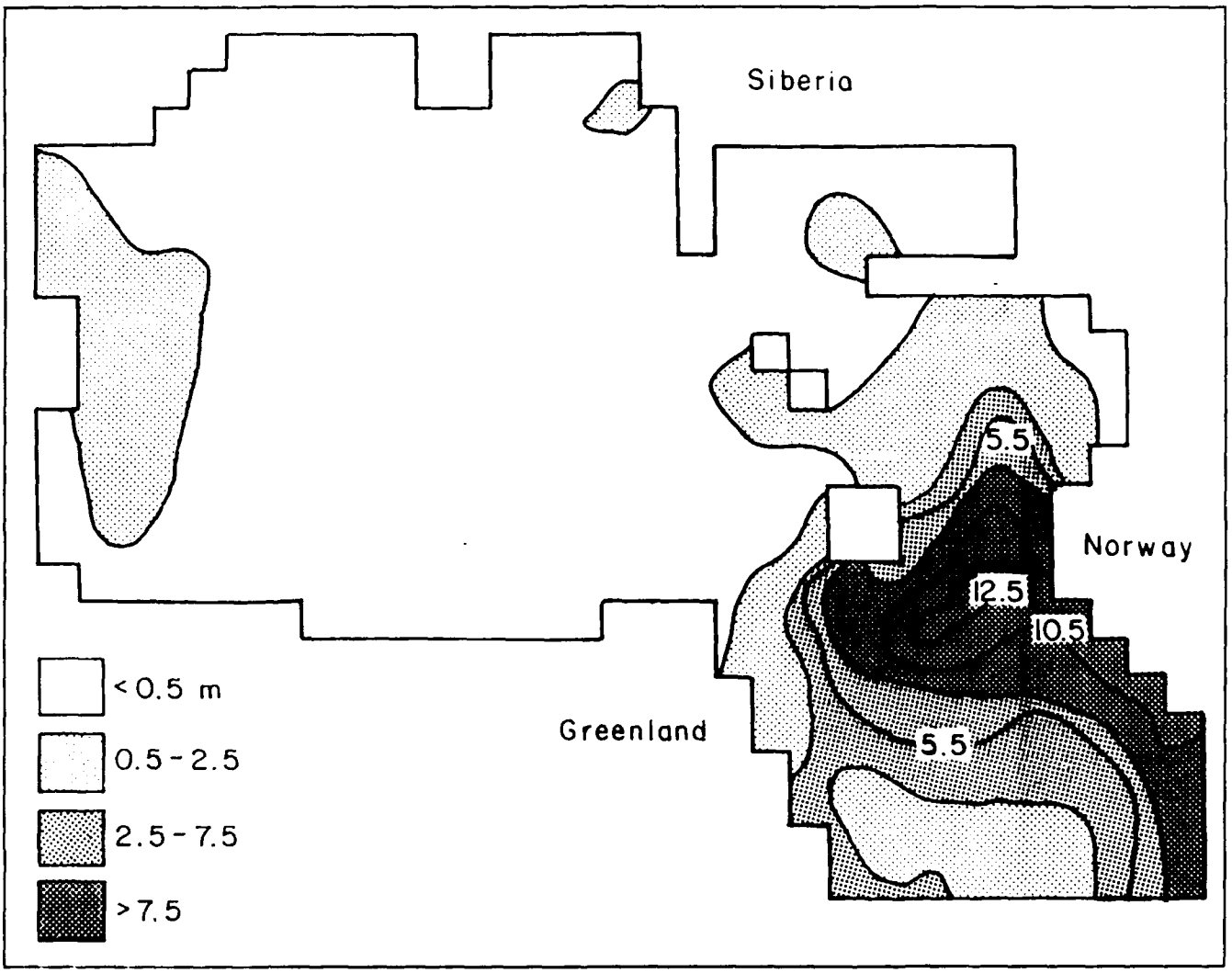

Figure 3. Average annual heat gained by the upper layer of the ocean from the deeper ocean and lateral heat transport. Contours are in capacity of heat used to melt meters of ice per year (1 m/year = 9.57 W-m^2) from Hibler and Bryan (1987).

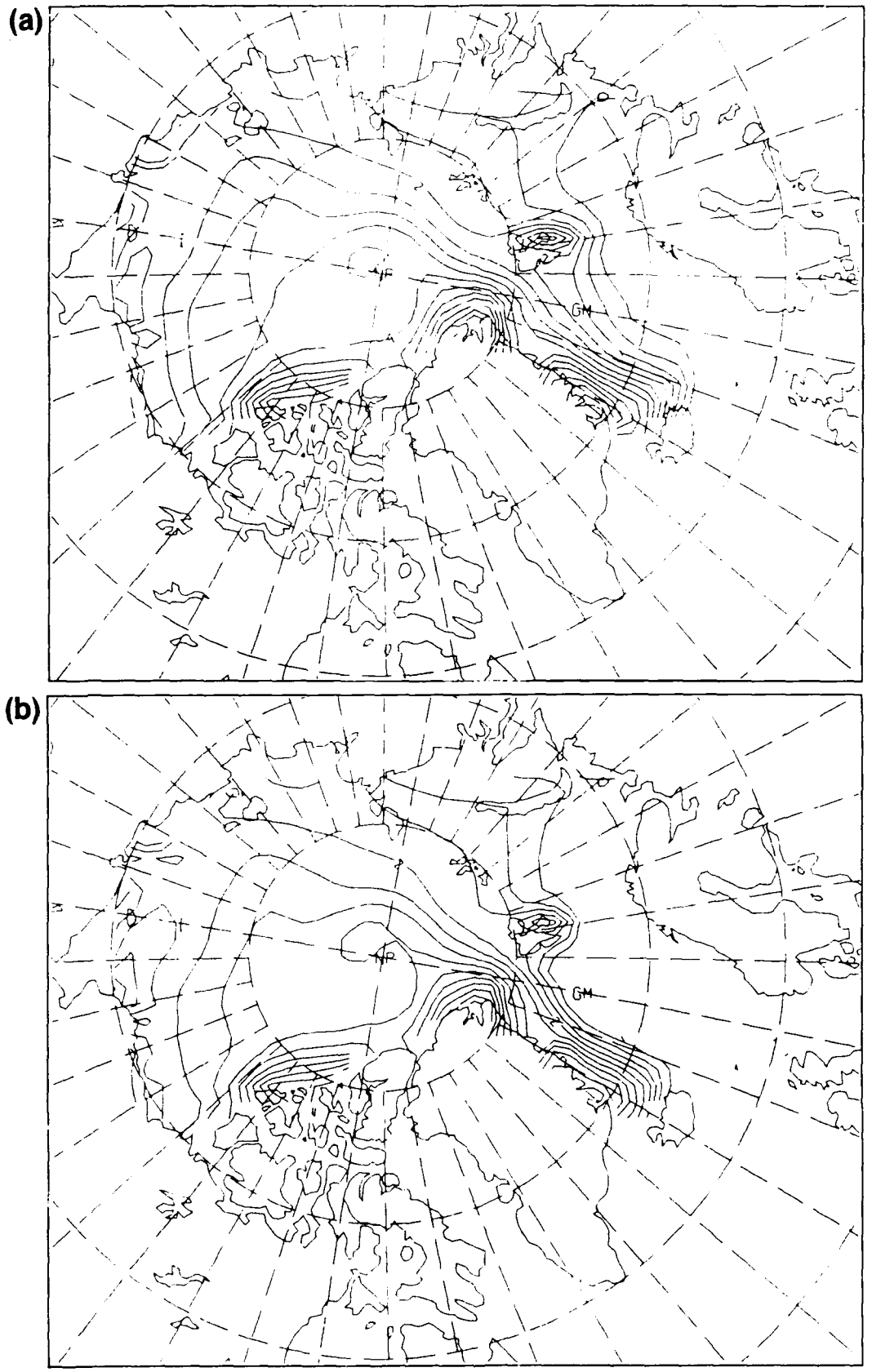

Figure 4. Model simulated ice thickness using (a) constant oceanic heat flux of 2 W-m^{-2} (b) monthly mean Hibler-Bryan oceanic heat flux. The southernmost contour approximates the model ice edge. Contour interval is 0.5 m.

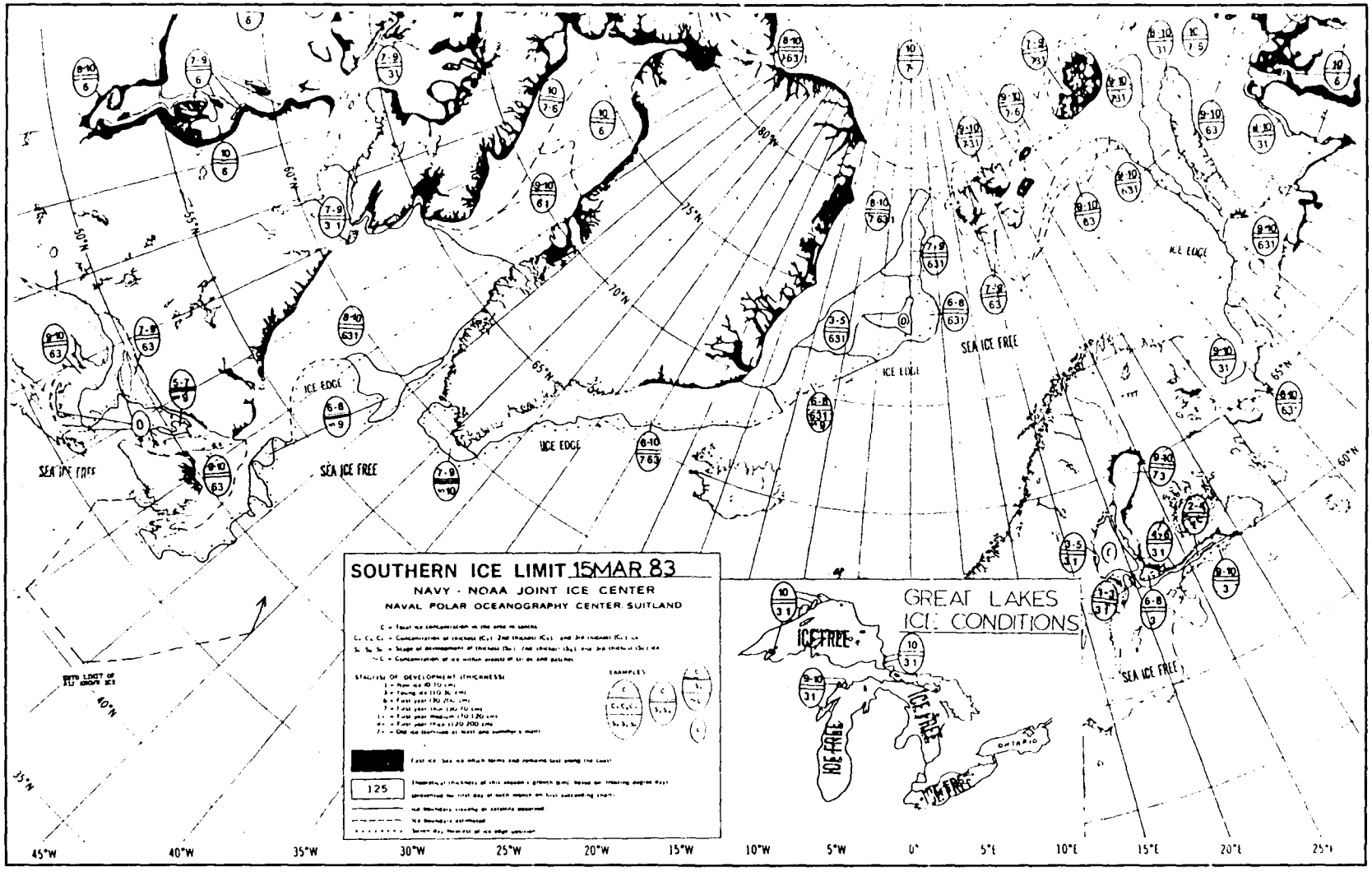

Figure 5. Navy/NOAA Joint Ice Center analysis of ice concentration for the eastern Arctic on 15 March 1983.

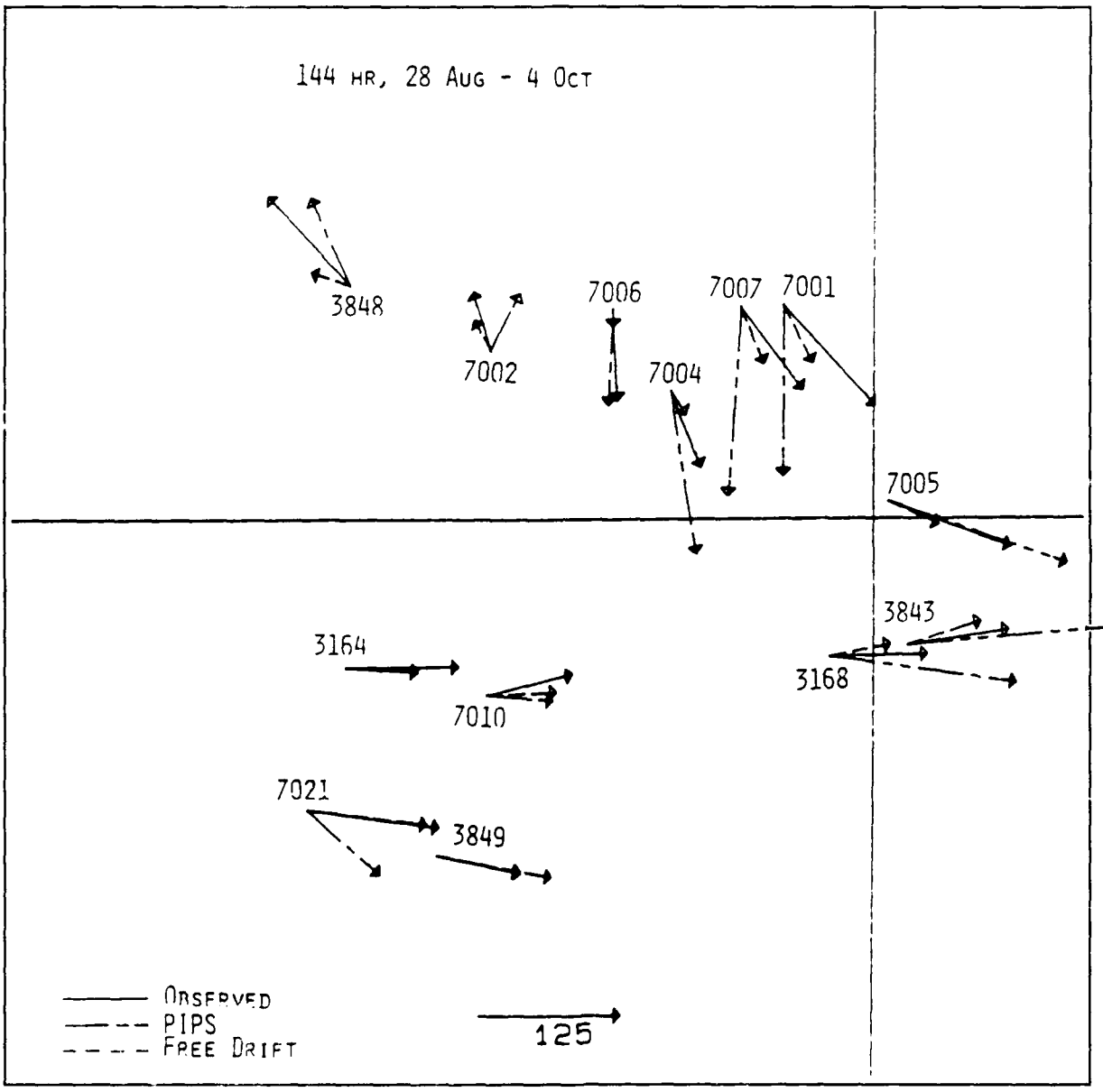

Figure 6. The 144 hour cumulative ice drift from 10 chosen forecast days during the period 28 August—4 October 1986. Results are from buoys, the free-drift models, and PIPS. Scale is in nautical miles.

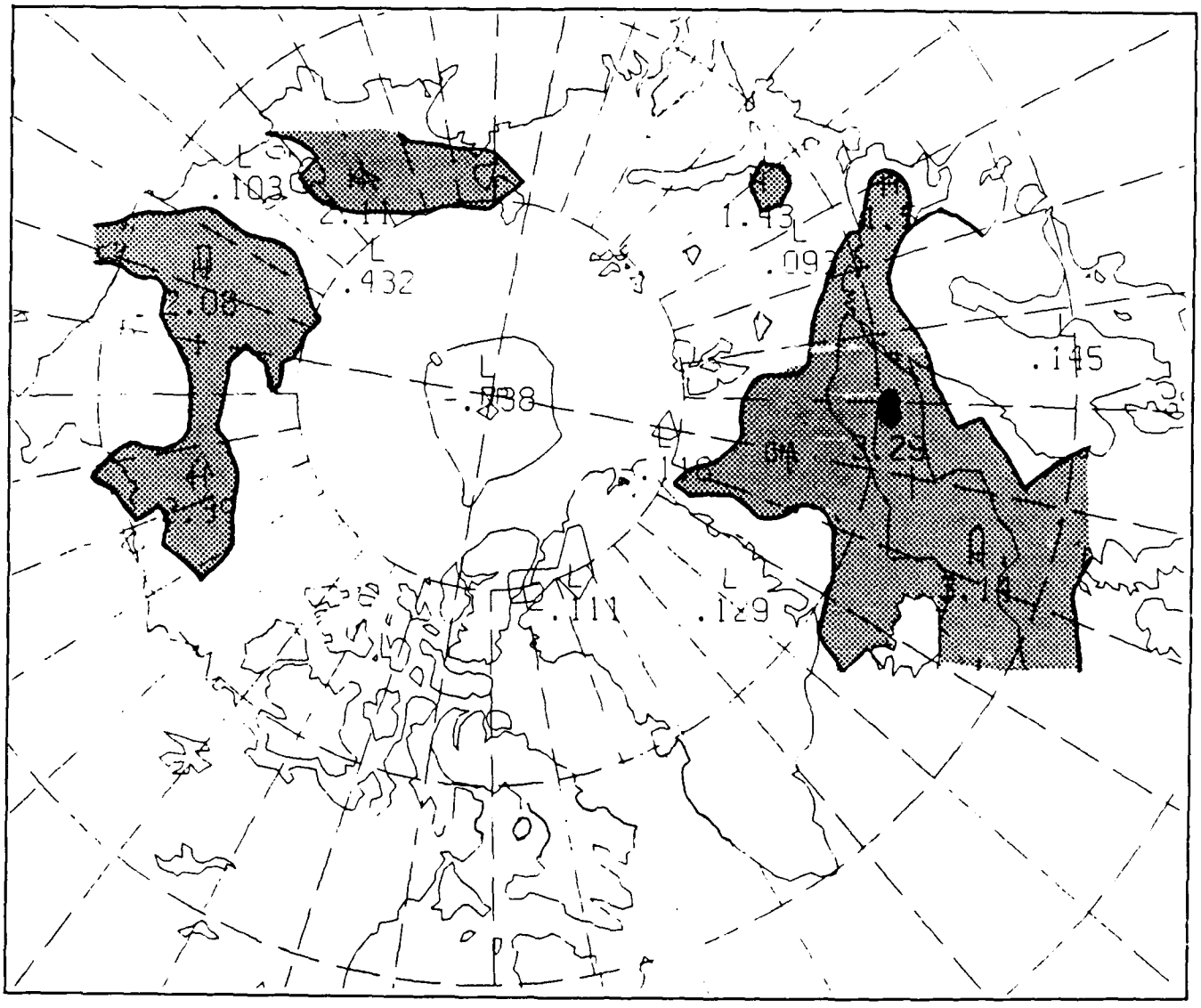

Figure 7. Difference between Marine Boundary Layer Wind Stress and Geostrophic Wind Stress averaged over an 8-day period in May 1983. Contours are 1 dyne/cm². Shaded areas are differences greater than 1 dyne/cm².

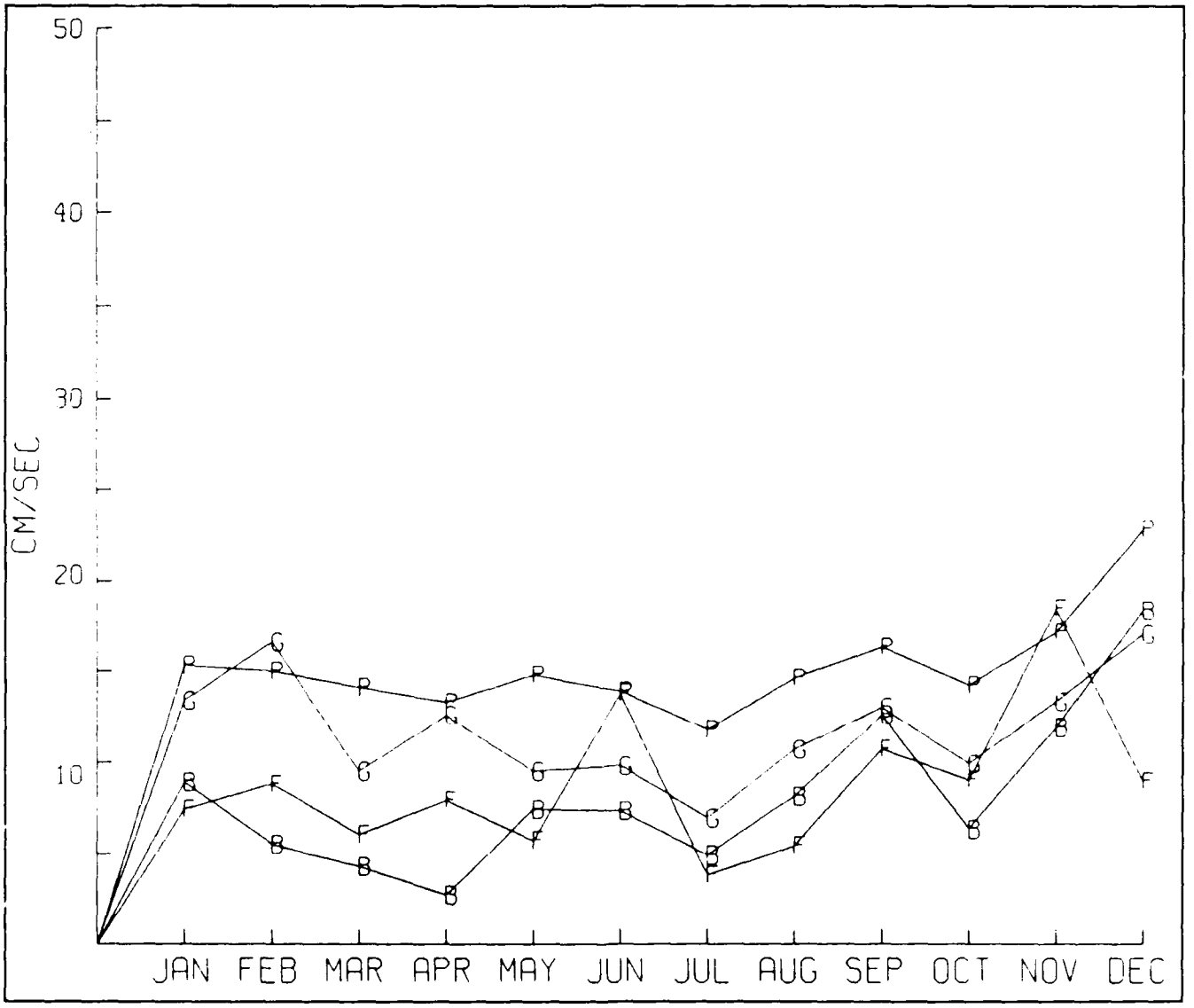

Figure 8. Monthly mean ice drift magnitude averaged over every available buoy location. "P" represents PBLNH wind result. "G" is geostrophic wind result, "F" is the free-drift result, and "B" is buoy data.

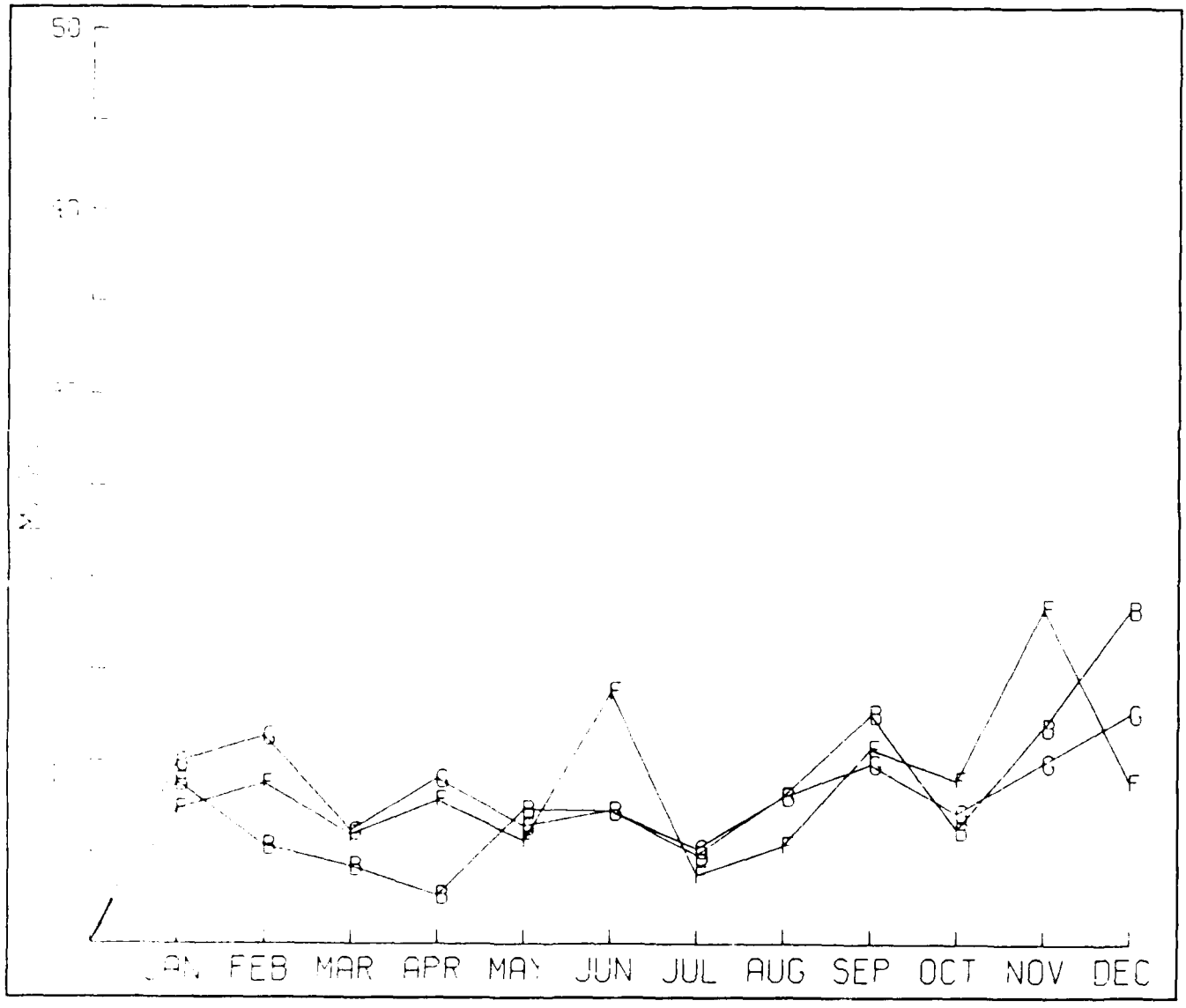

Figure 9. Monthly mean ice drift magnitude averaged over every available buoy location. "G" is the geostrophic wind result using a 0.8 x 10^{-3} drag coefficient; "F" and "B" are the free-drift and buoy results (same as Fig. 8).

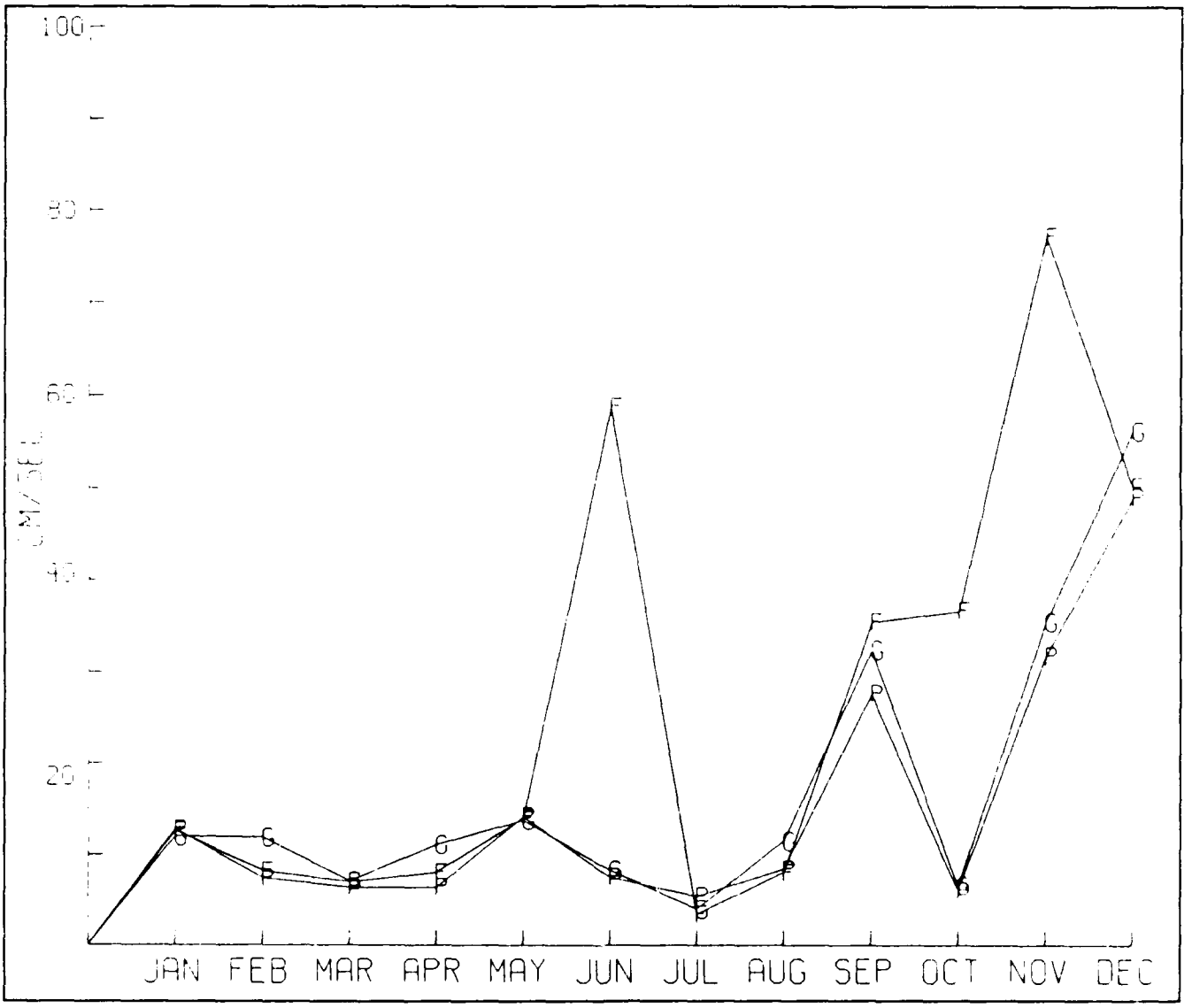

Figure 10. Monthly mean RMS error for ice drift magnitude for the "G" geostrophic wind case (0.8 × 10 ⁻³) and the "F" free-drift case.

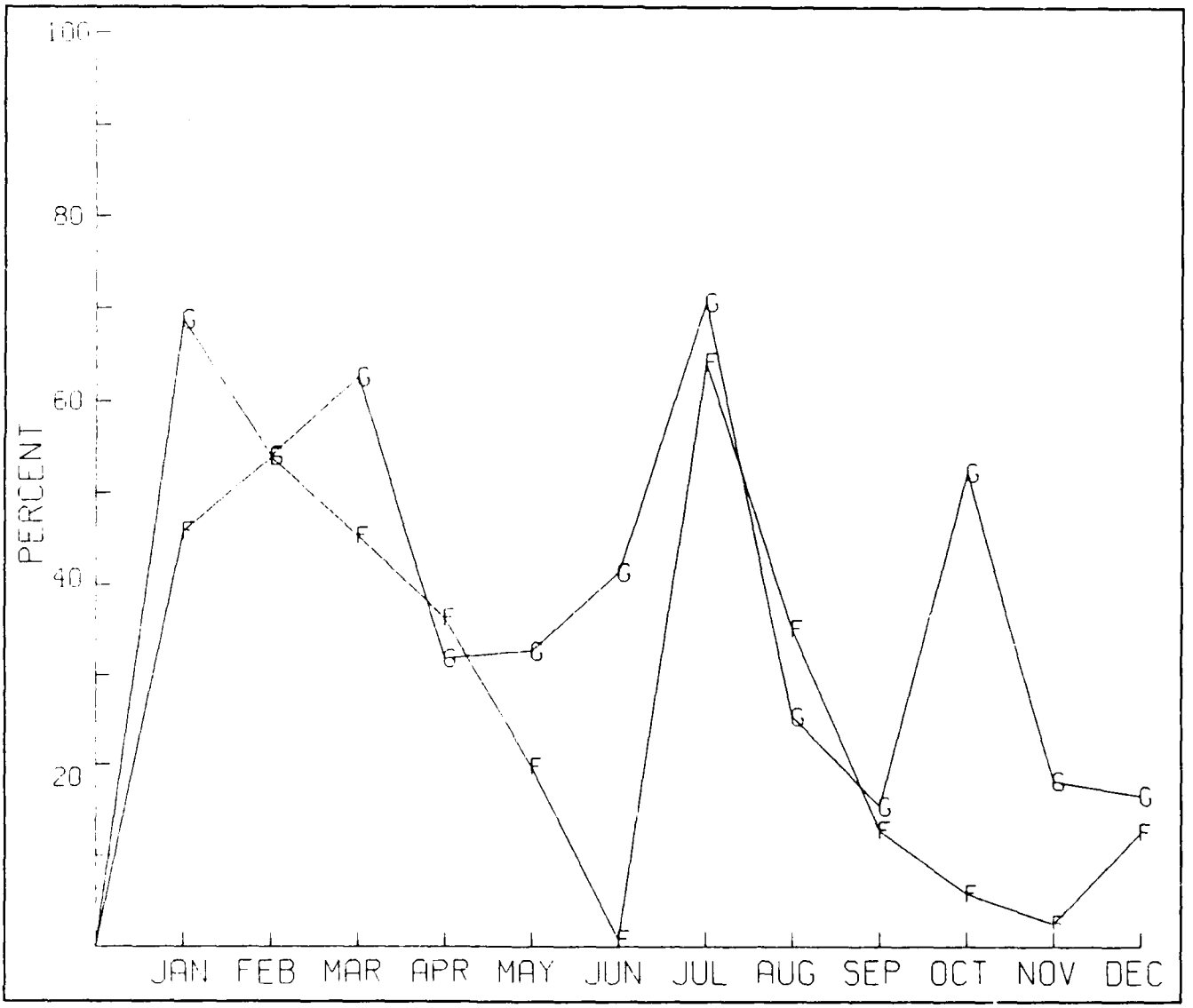

Figure 11. Monthly mean index of agreement for ice drift magnitude averaged over every buoy for the "G" geostrophic wind case and the "F" free-drift case.

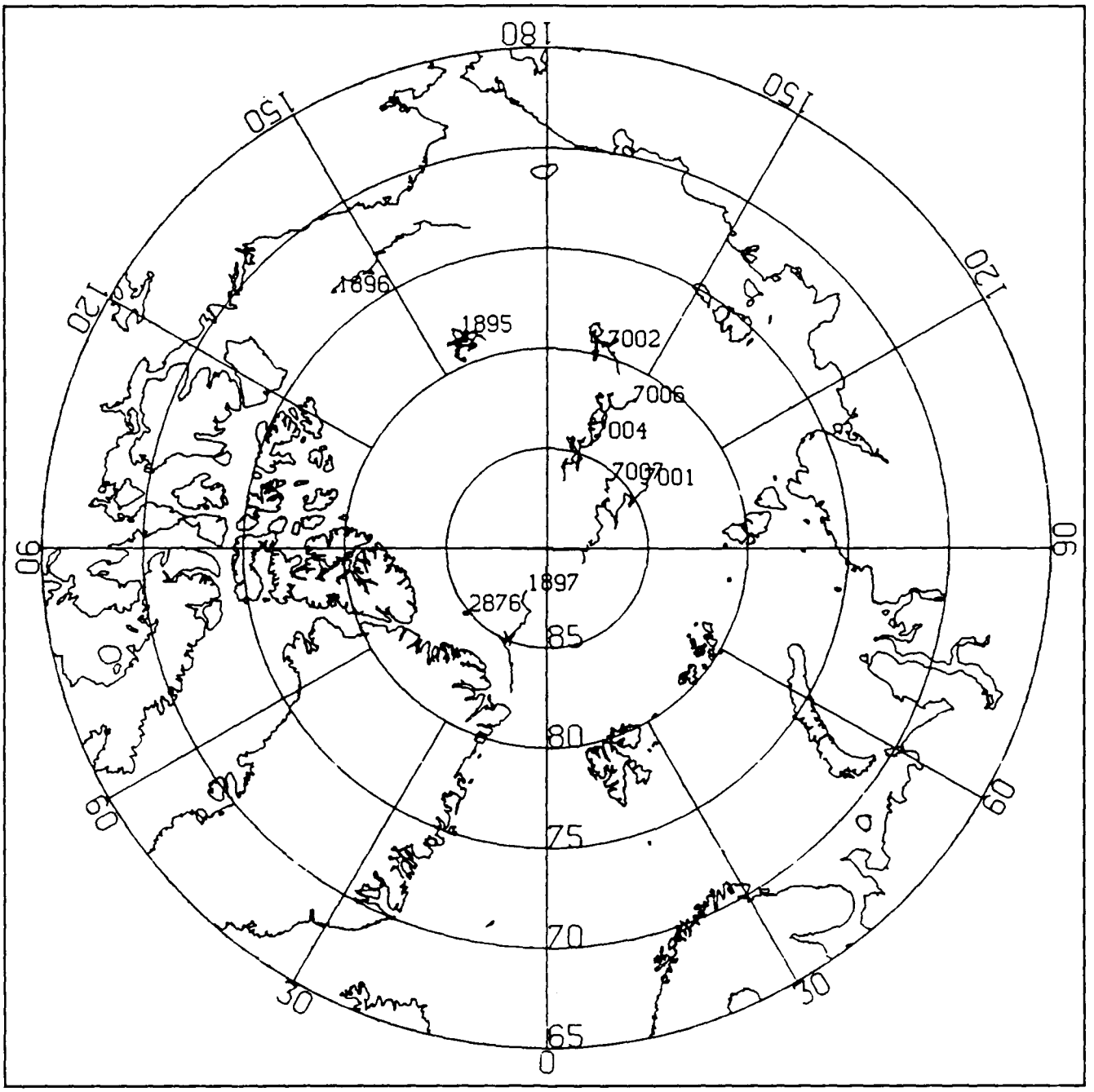

Figure 12. Arctic buoys available during June 1987.

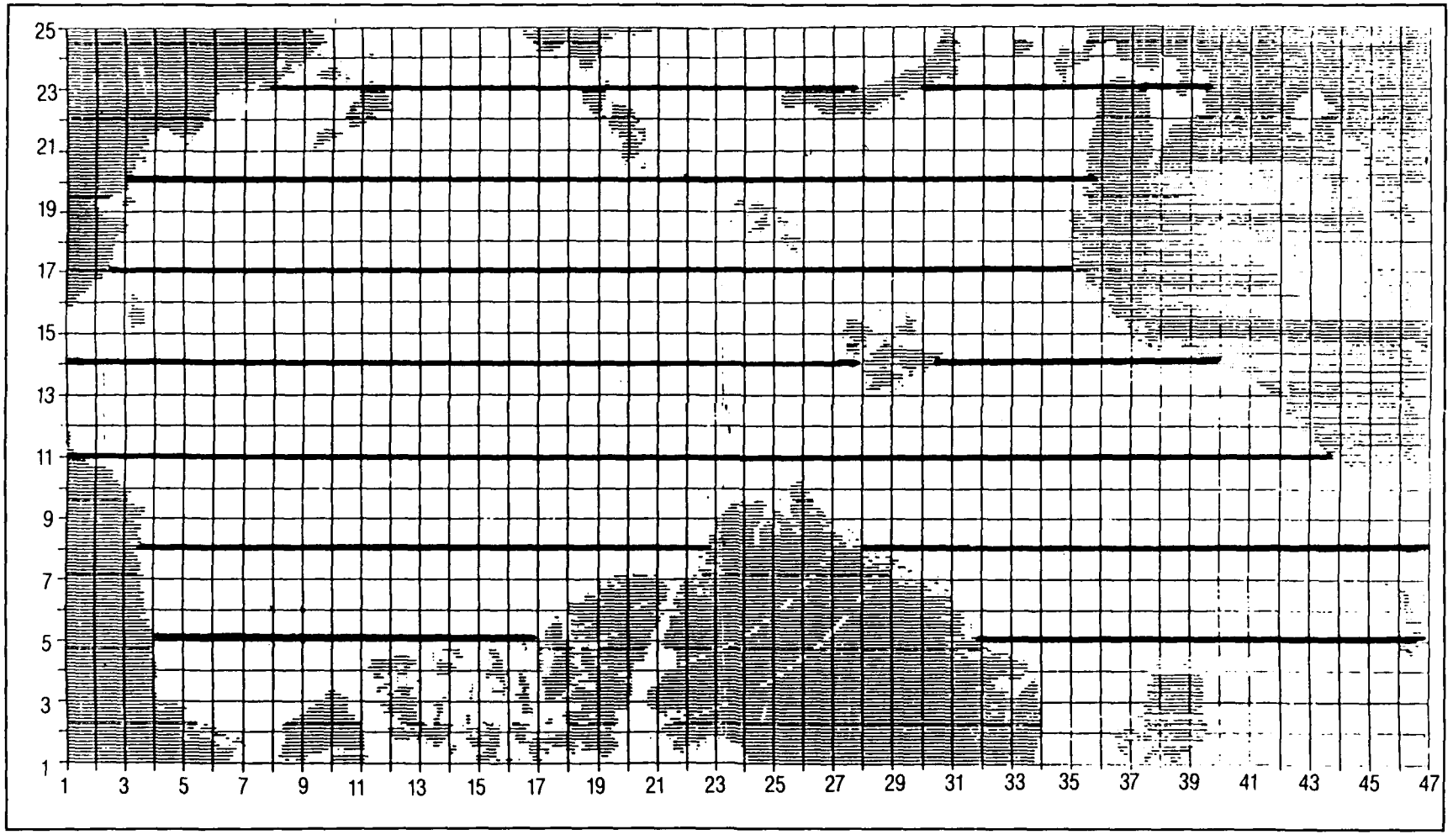

Figure 13. PIPS model grid. Line used in concentration and edge location analysis are highlighted.

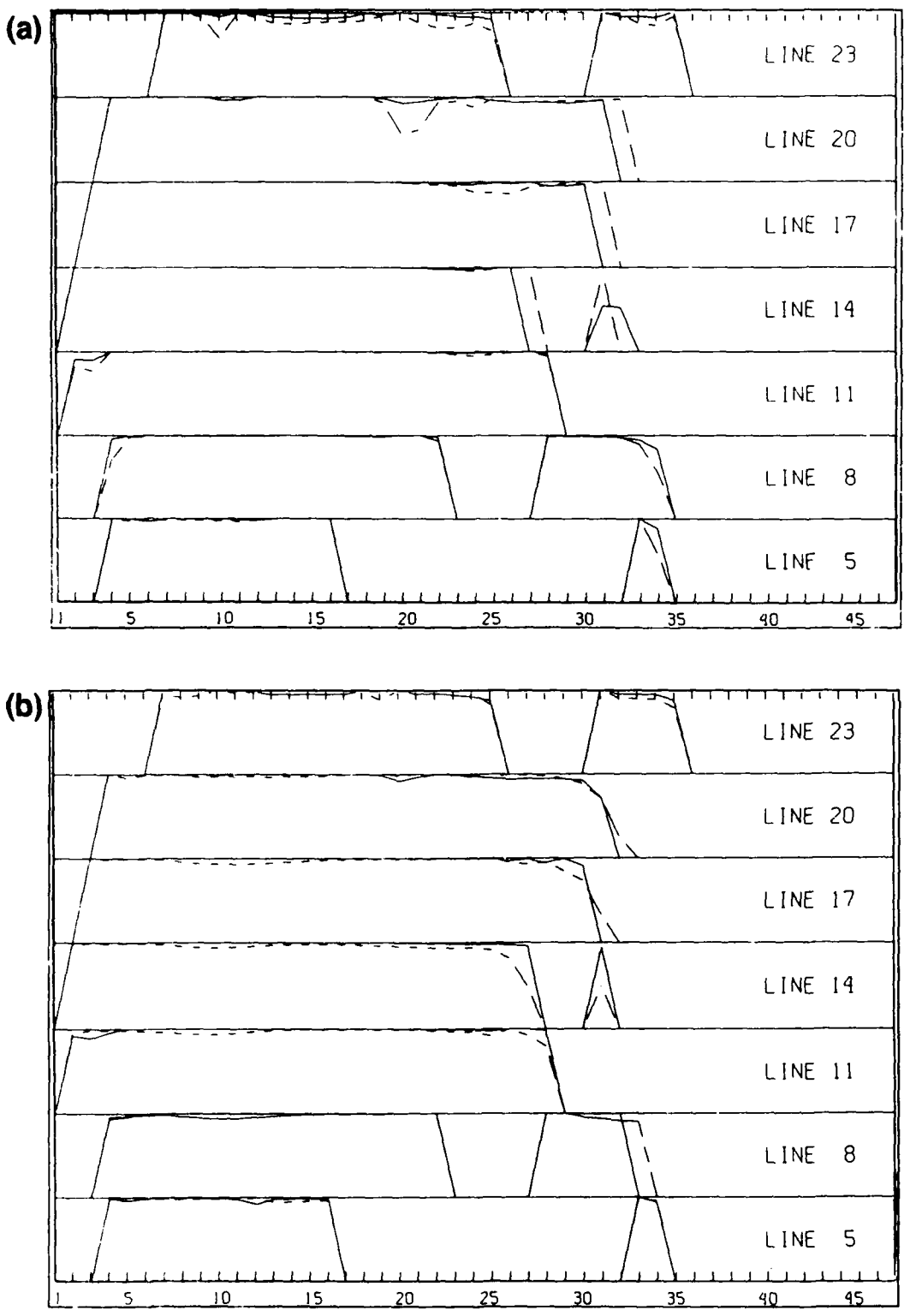

Figure 14. Ice concentration along each line shown in Figure 13 from the model (dashed) and from NPOC analysis (solid). Winter comparison for (a) 10 April 1987 and (b) 30 April 1987. Both cases were updated 7 days prior to this result.

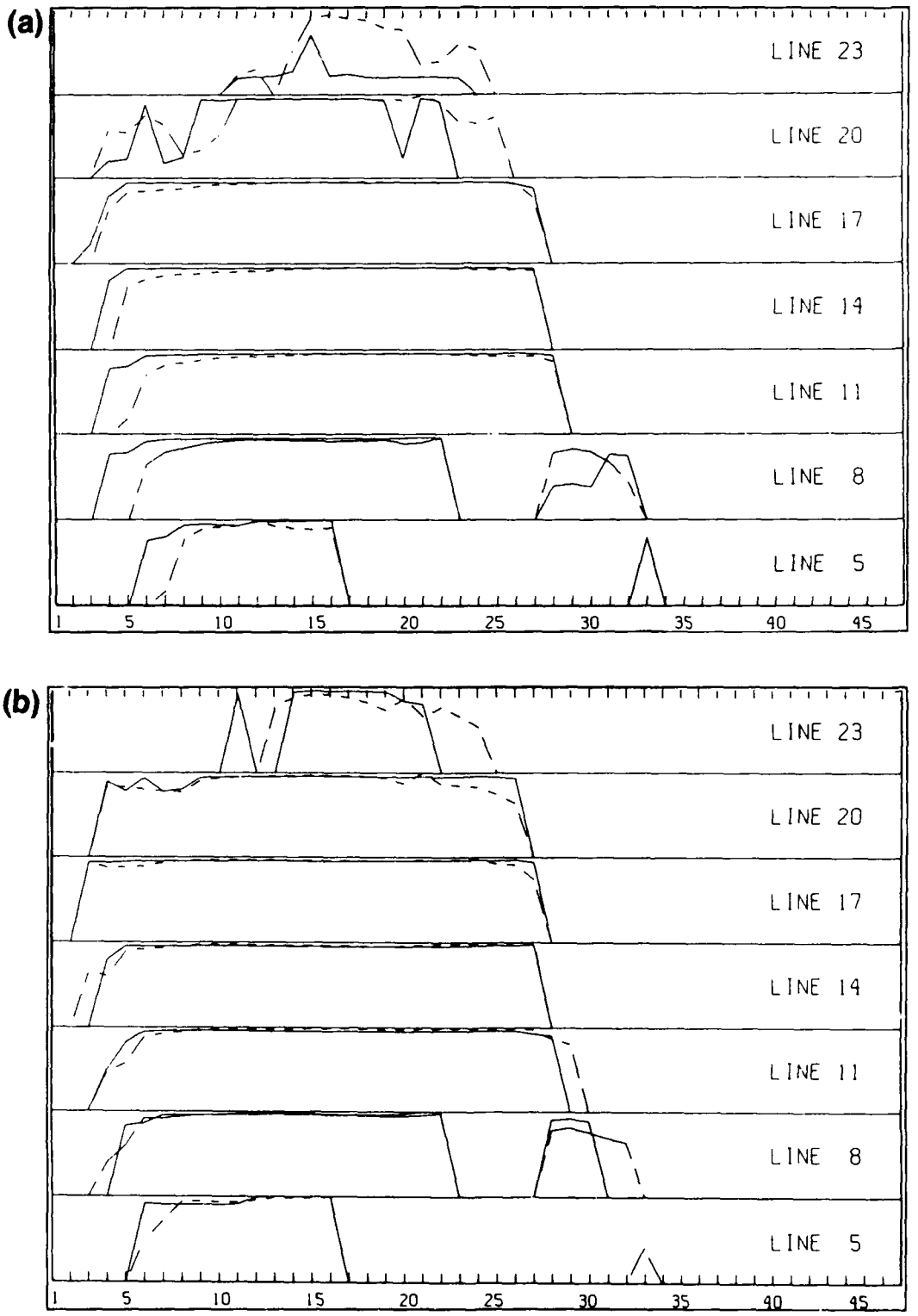

Figure 15. Ice concentration along each line shown in Figure 13 from model (dashed) and from NPOC analysis (solid). Summer comparison for (a) 11 September 1987 (7 days since update), (b) 2 October 1987 (21 days since update.

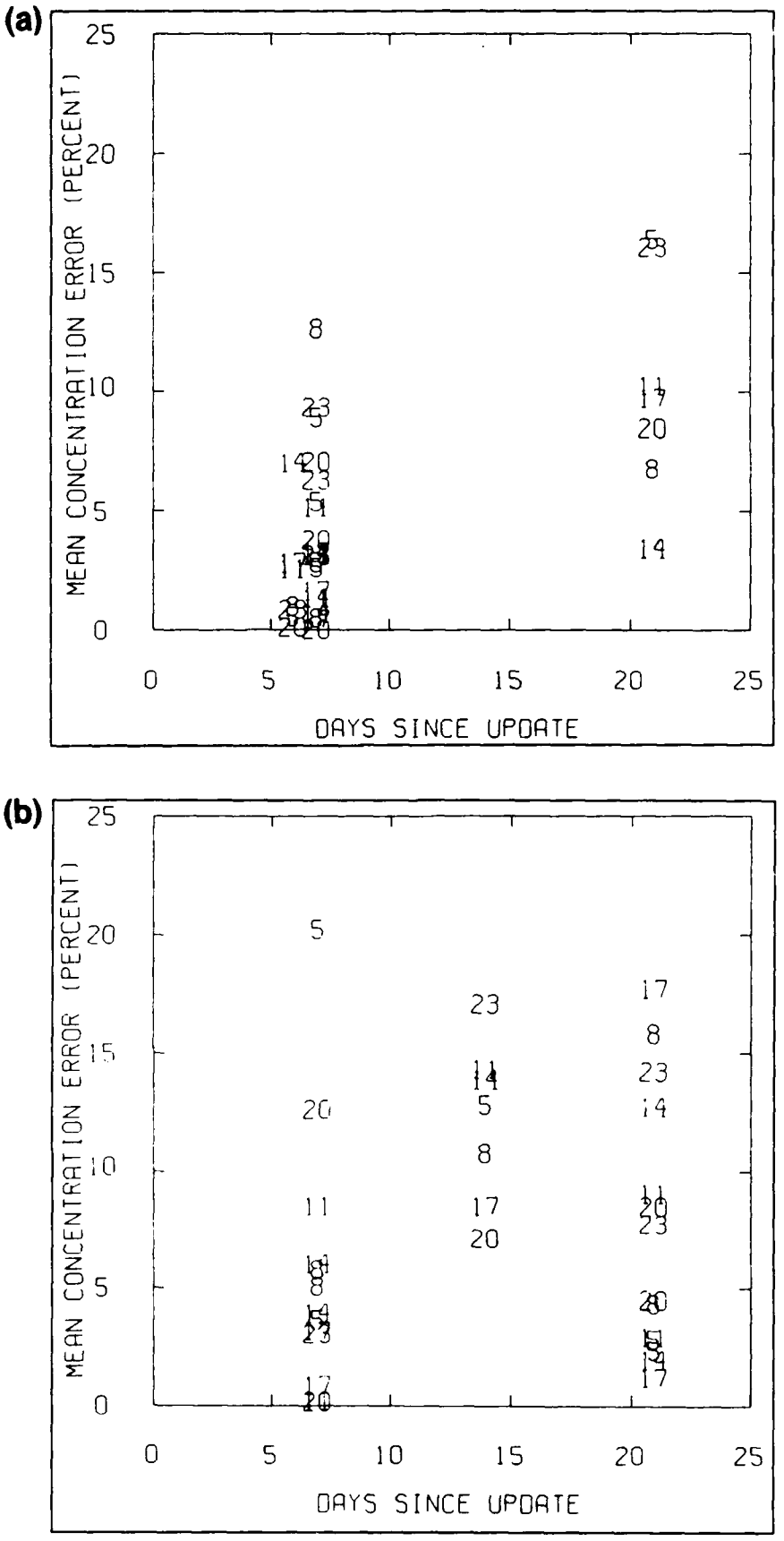

Figure 16. Mean concentration error along each line versus the number of days since an update for (a) 5 winter cases and (b) 5 summer cases.

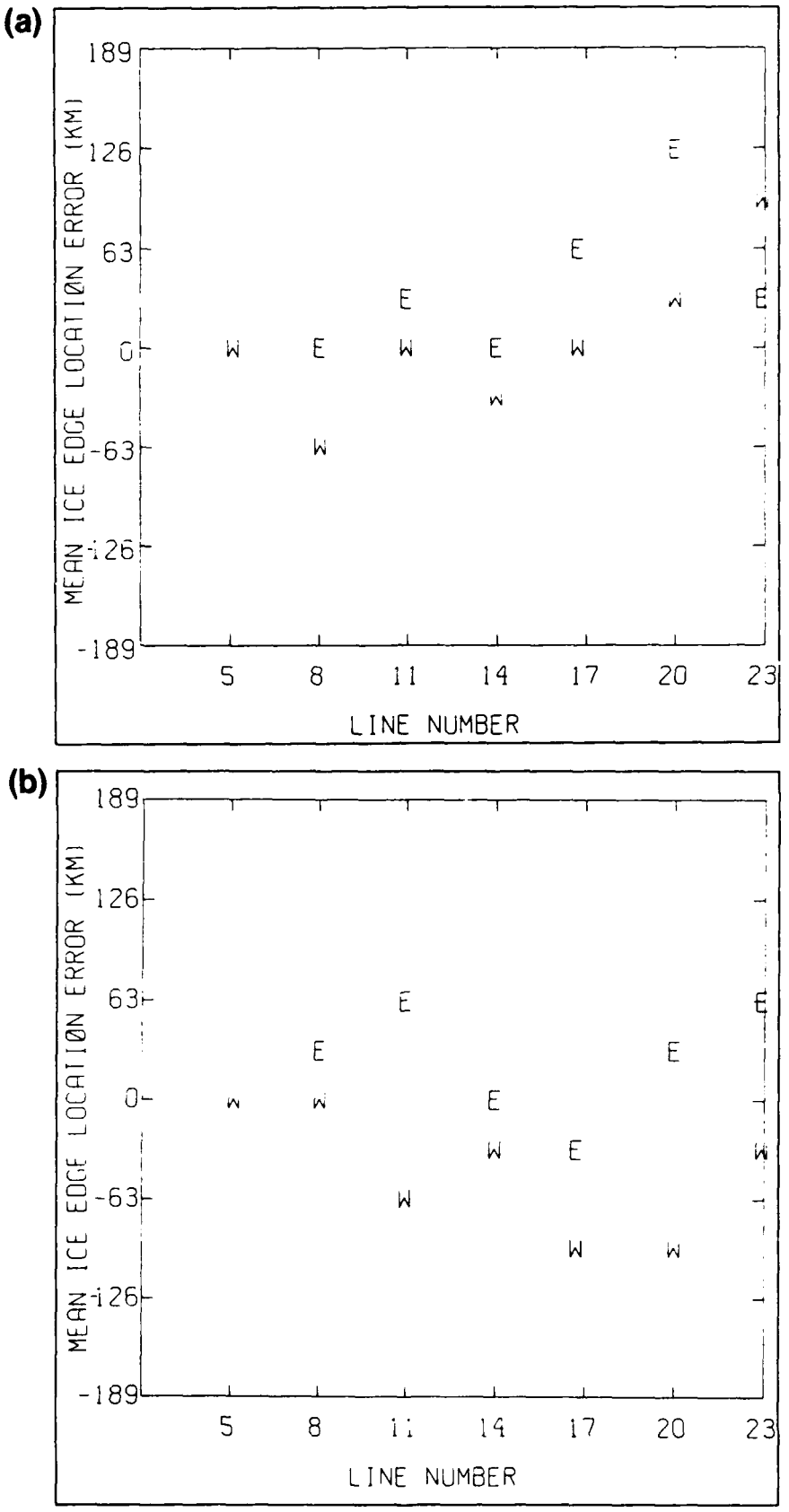

Figure 17. Mean ice edge error (model-data) averaged for (a) two "7 days since update" cases and (b) two "21 days since update" cases in summer. "E" indicates error in eastern Arctic ice edge and "W" is the error in the western Arctic ice edge.

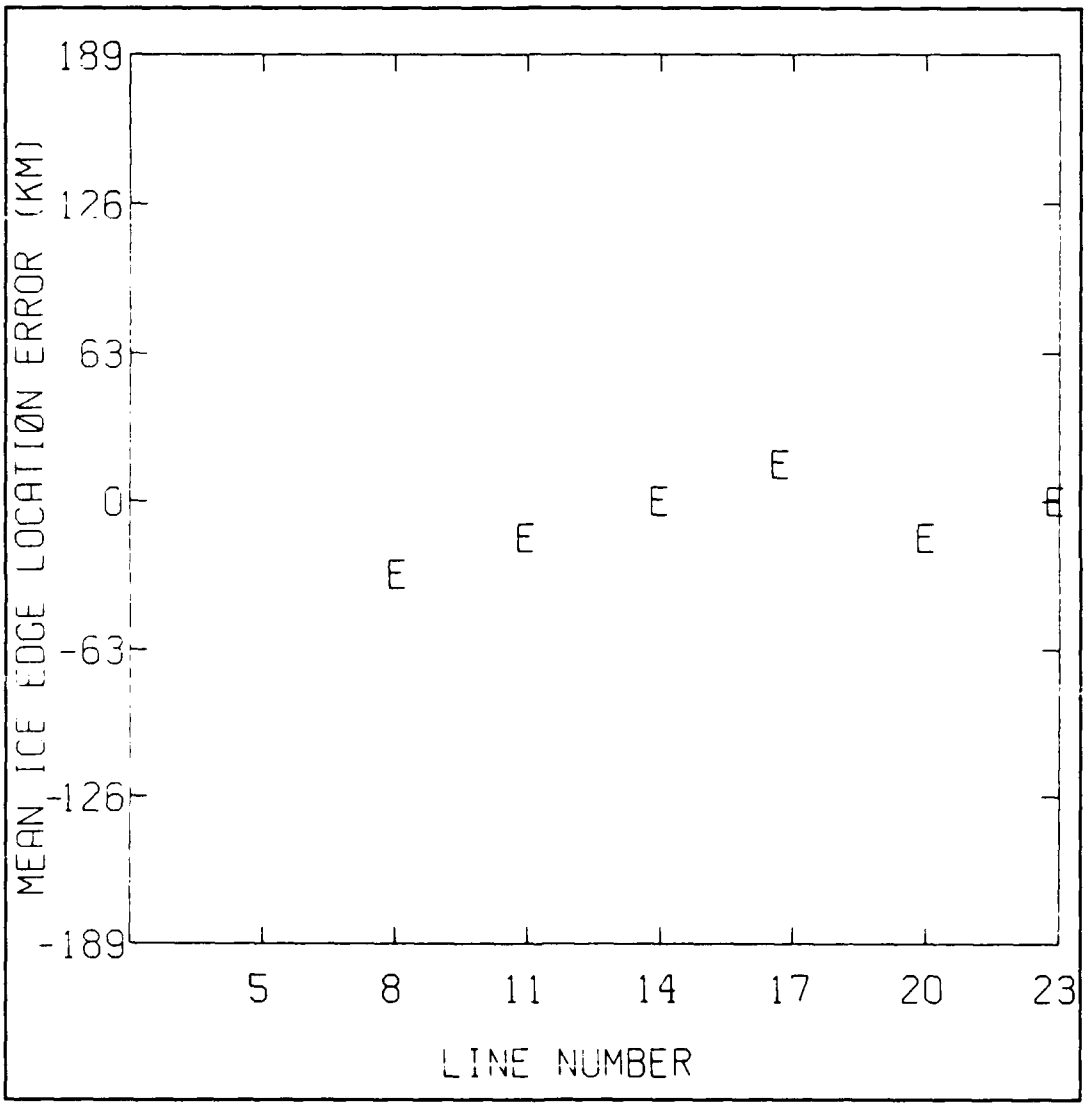

Figure 18. Mean ice edge error (model-data) averaged over four "7 days since update" cases in April, 1987. Due to the model boundary at the Bering Strait, only an Eastern Arctic ice edge exists in the model.

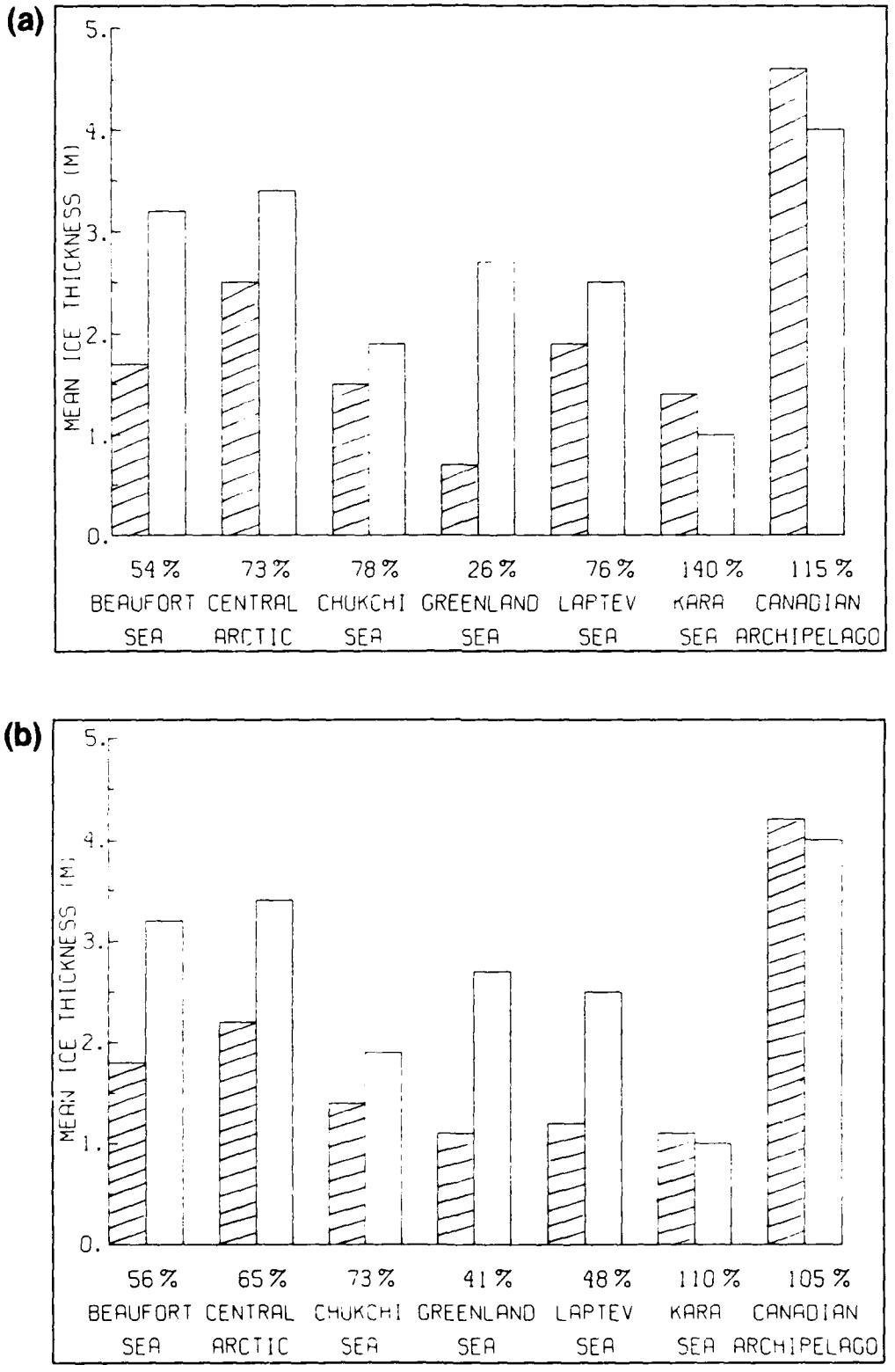

Figure 19. Regional mean ice thickness (a) 1986 PIPS vs. Garrett data (1985) and (b) 1987 PIPS vs. Garrett data. Hatched results are from the model. Percentage values are PIPS thickness divided by observed thickness and then multiplied by 100.

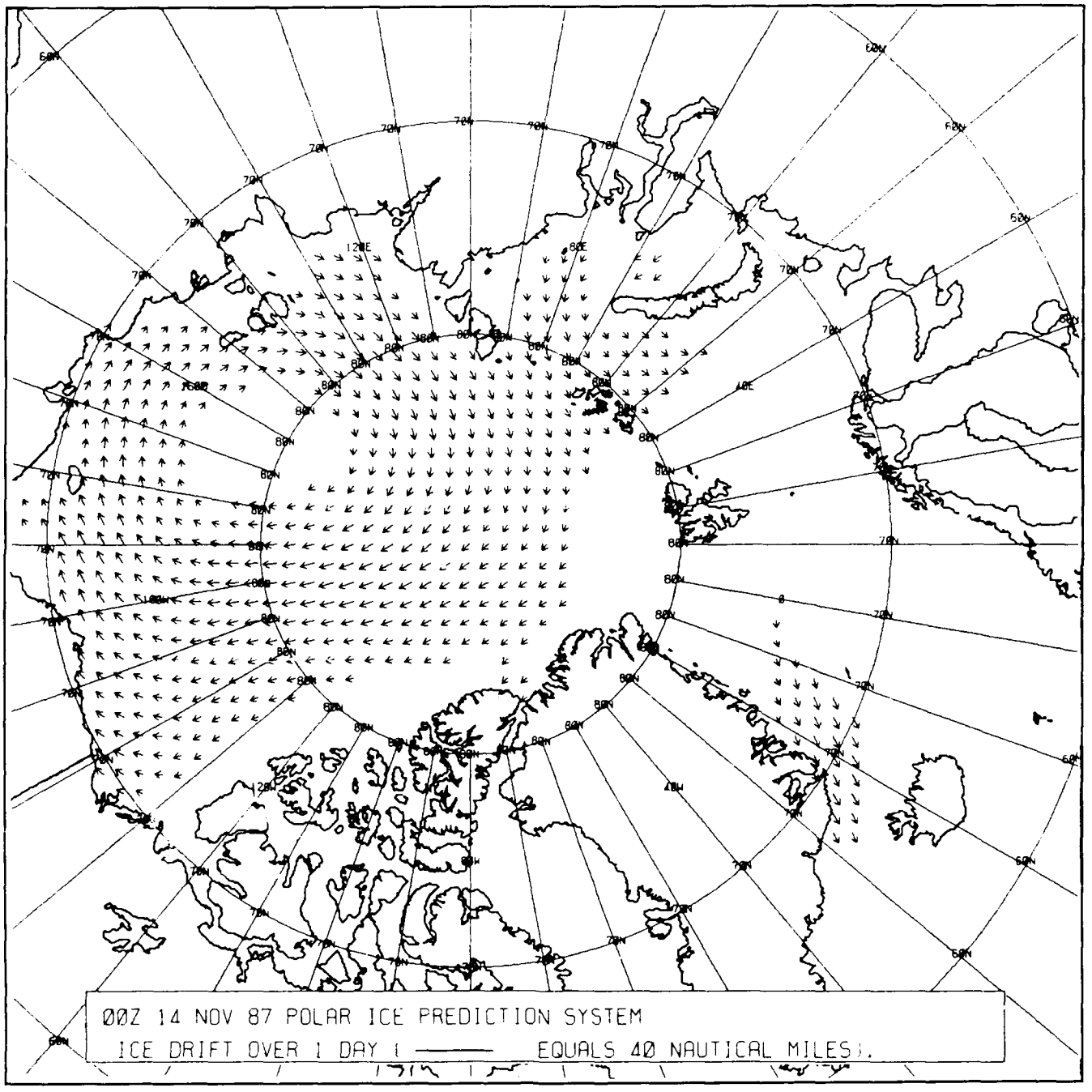

Figure 20a. PIPS Tau 24 cumulative ice drift from the 00Z 14 November 1987.

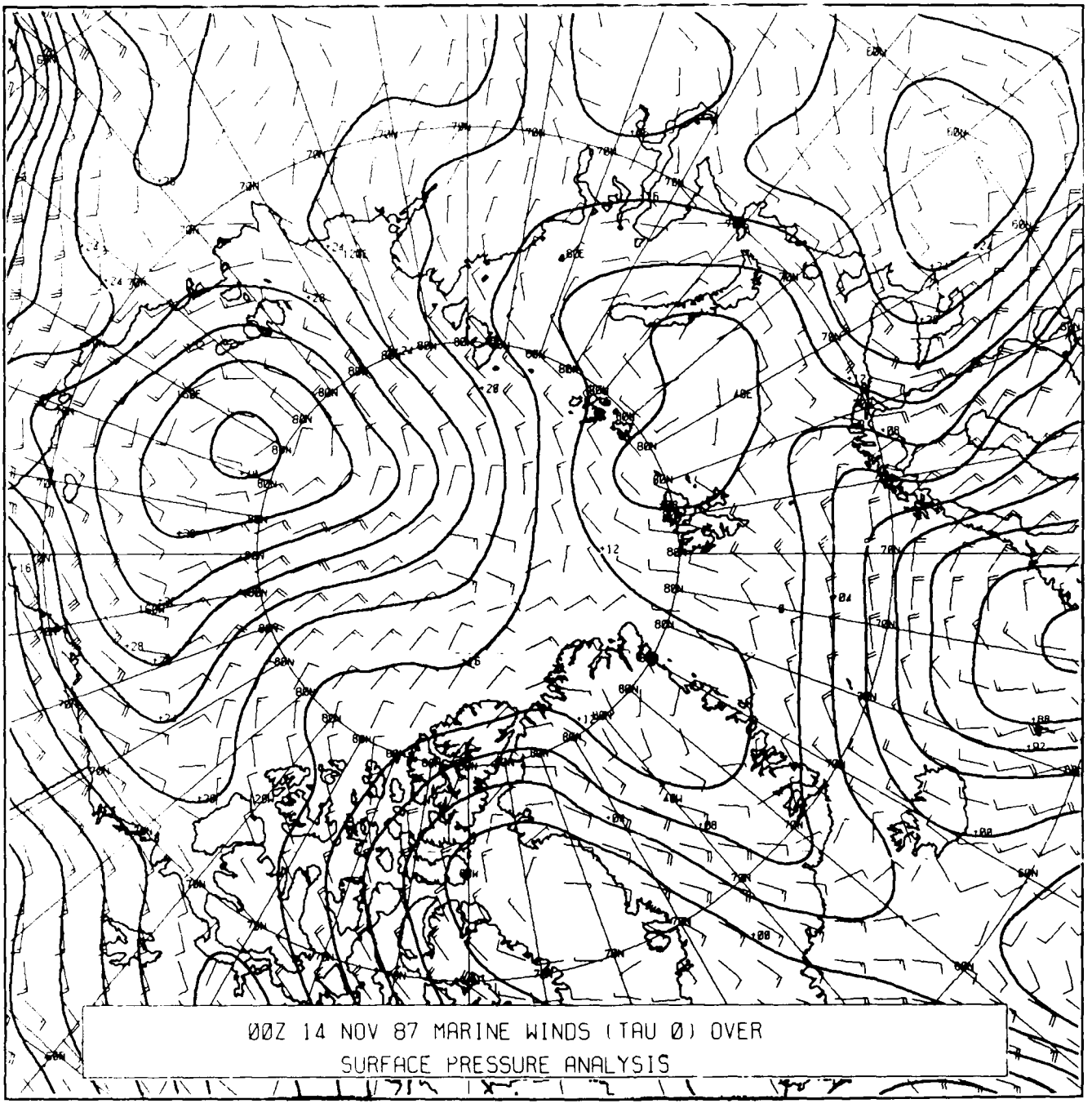

Figure 20b. NOGAPS Tau 0 surface pressure with PBLNH winds overlaid.

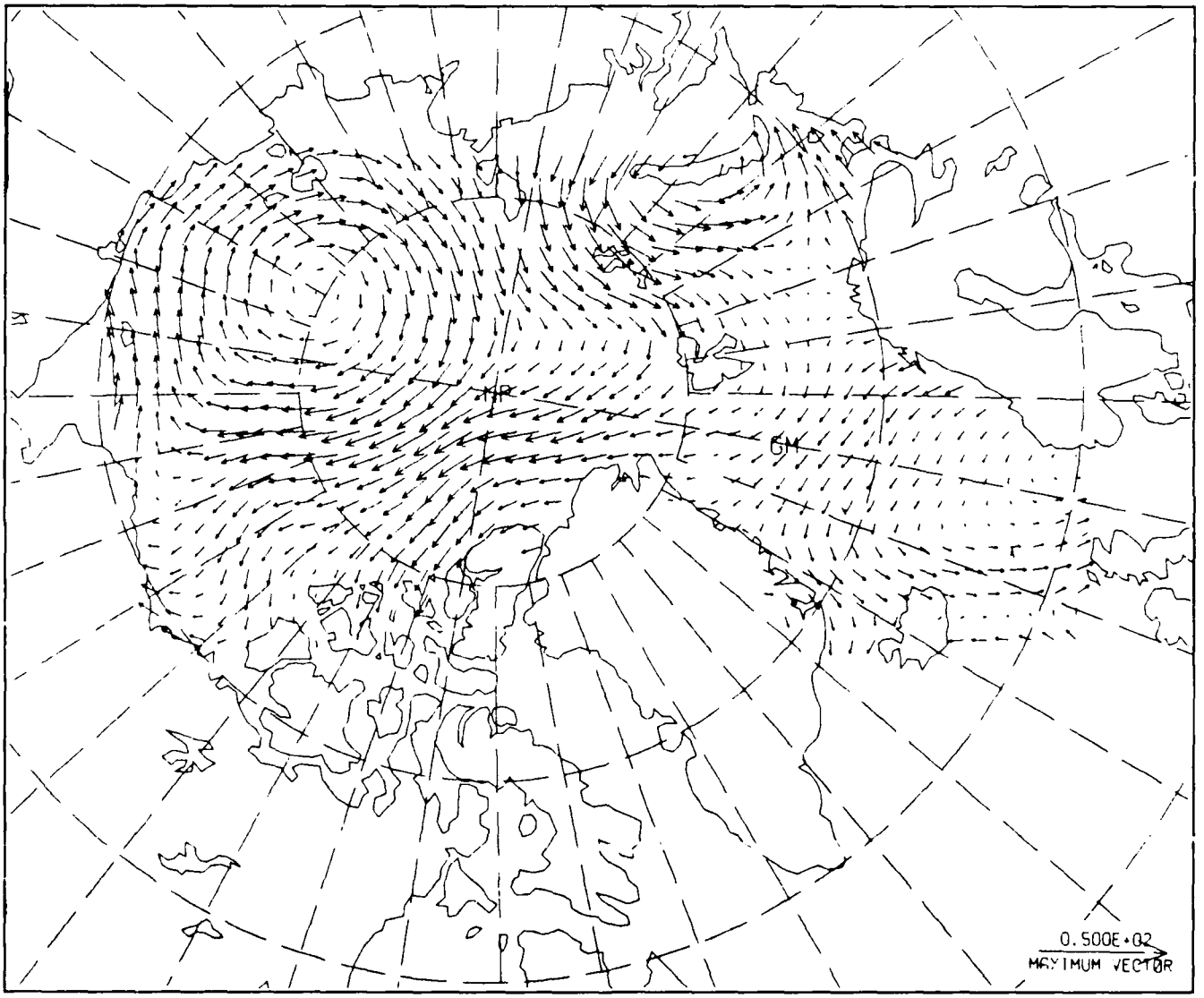

Figure 20c. Geostrophic wind calculated from the NOGAPS surface pressures.

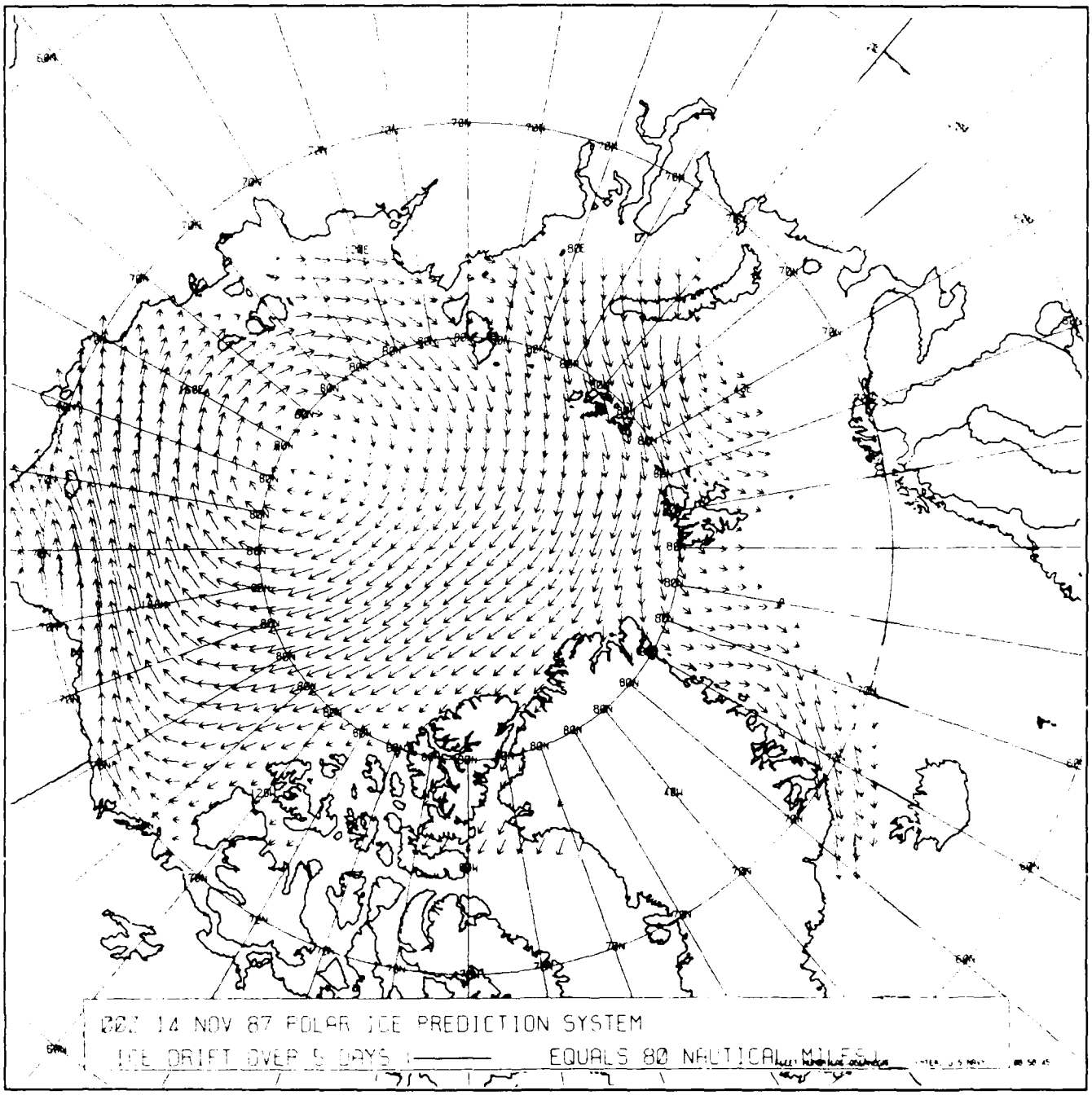

Figure 21a. PIPS 120-hour forecasted cumulative ice drift.

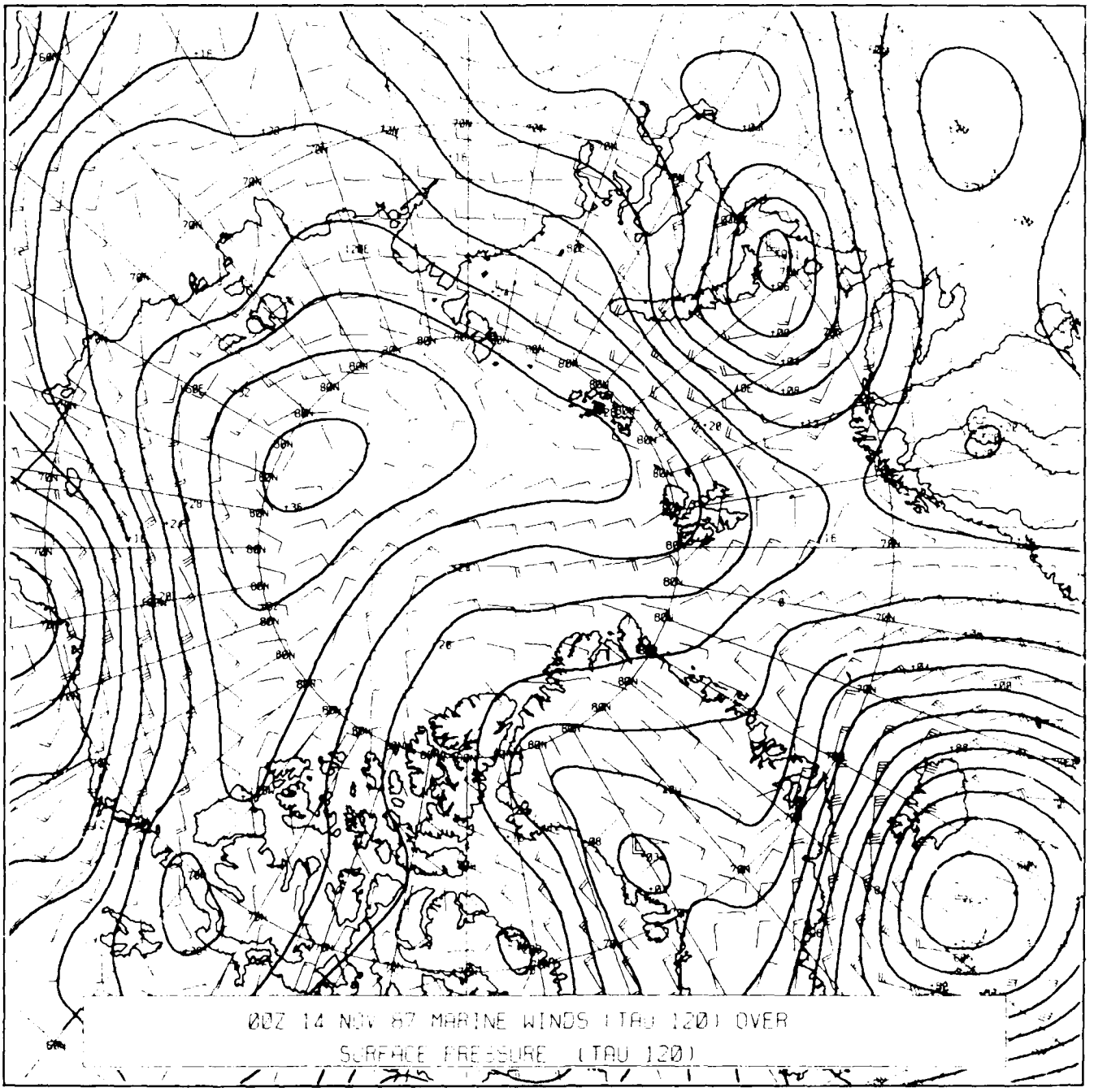

Figure 21b. Tau 120 NOGAPS surface pressures from the 14 November 1987 run.

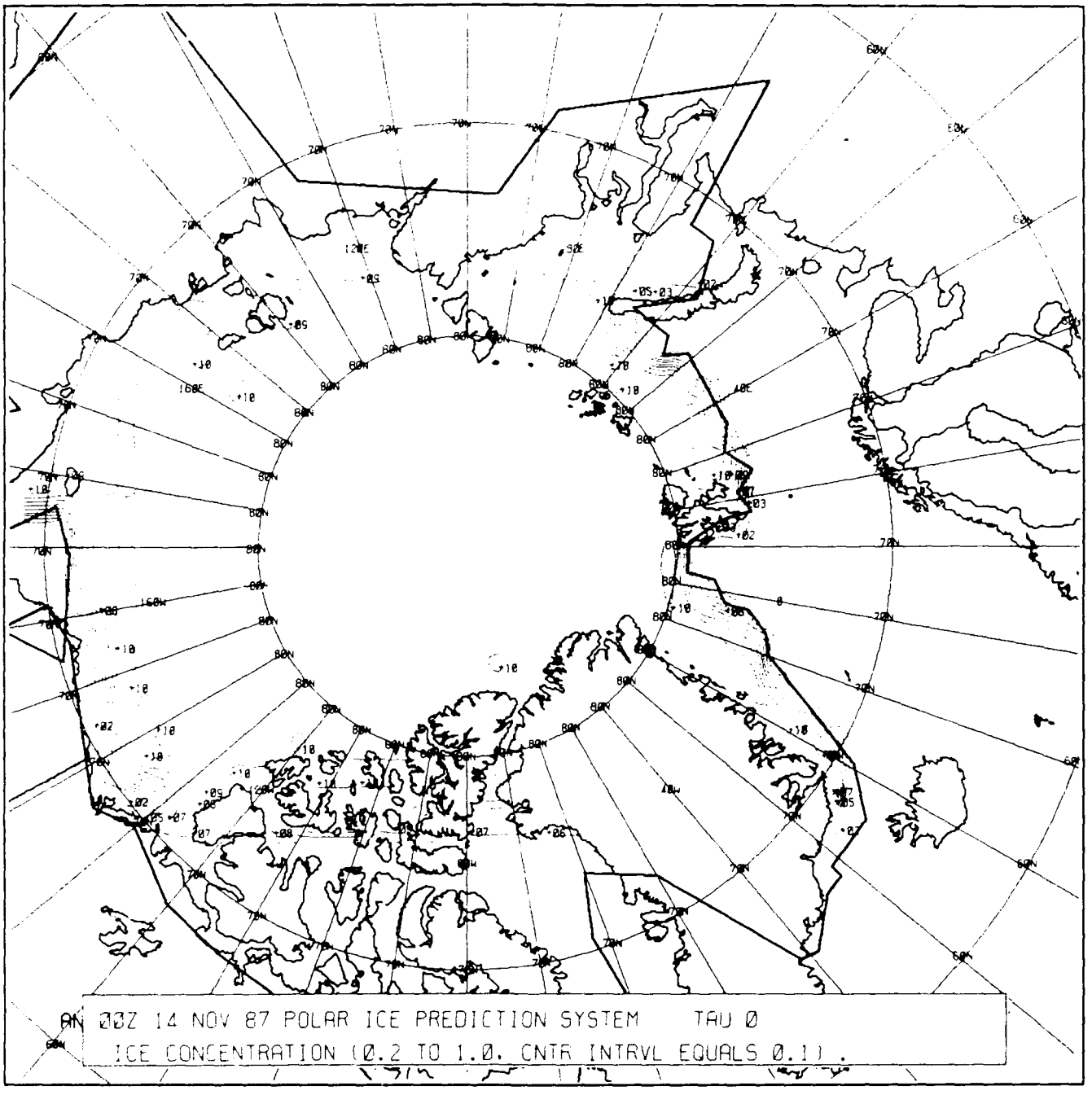

Figure 22a. PIPS Tau 0 ice concentration. Contour interval is 0.1 or 10%.

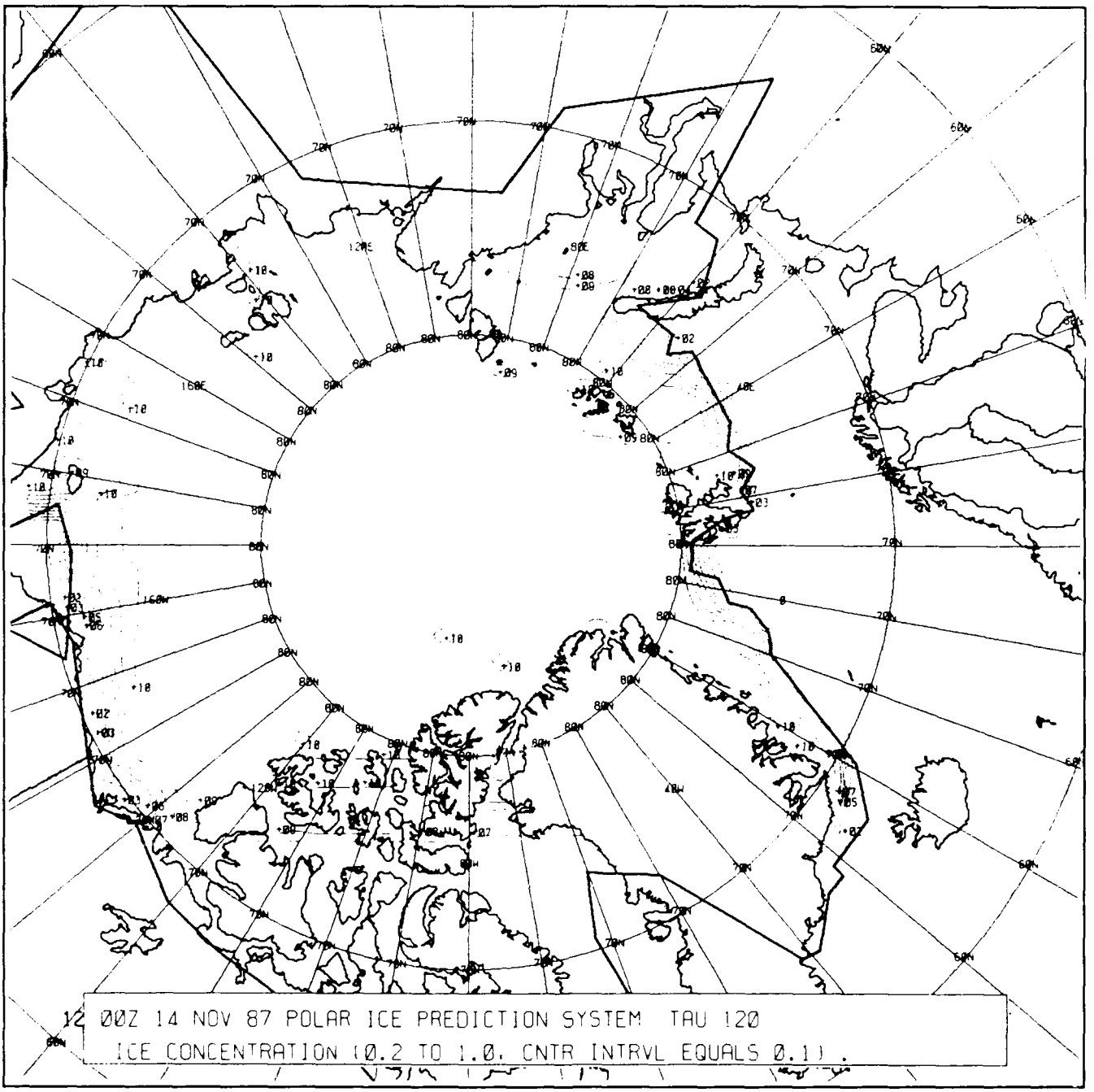

Figure 22b. Tau 120 forecasted ice concentration from the 17 November 1987 run. Contour interval is 0.1 or 10%.

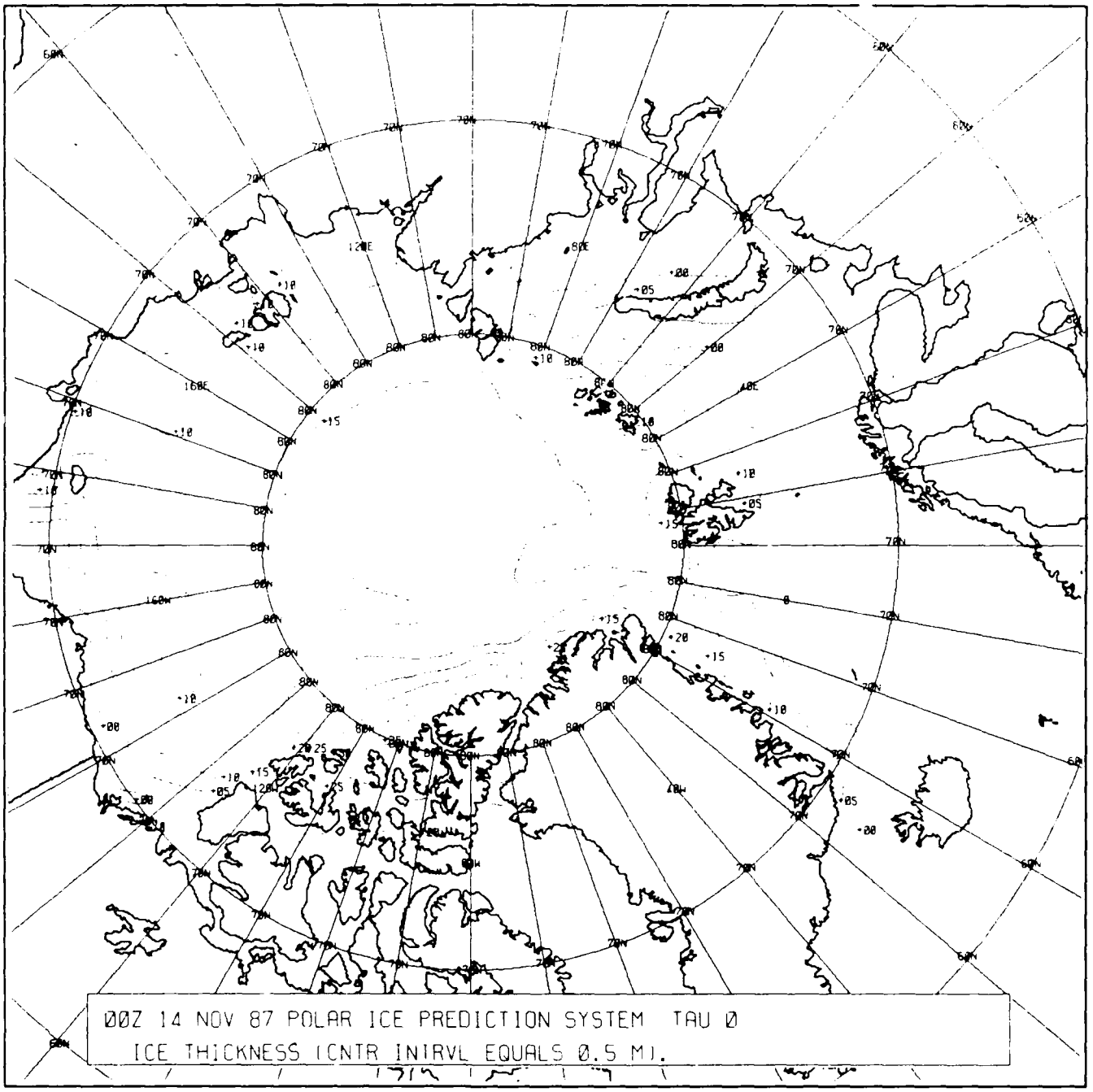

Figure 23a. PIPS Tau 0 ice thickness. Contour interval is 0.5 m.

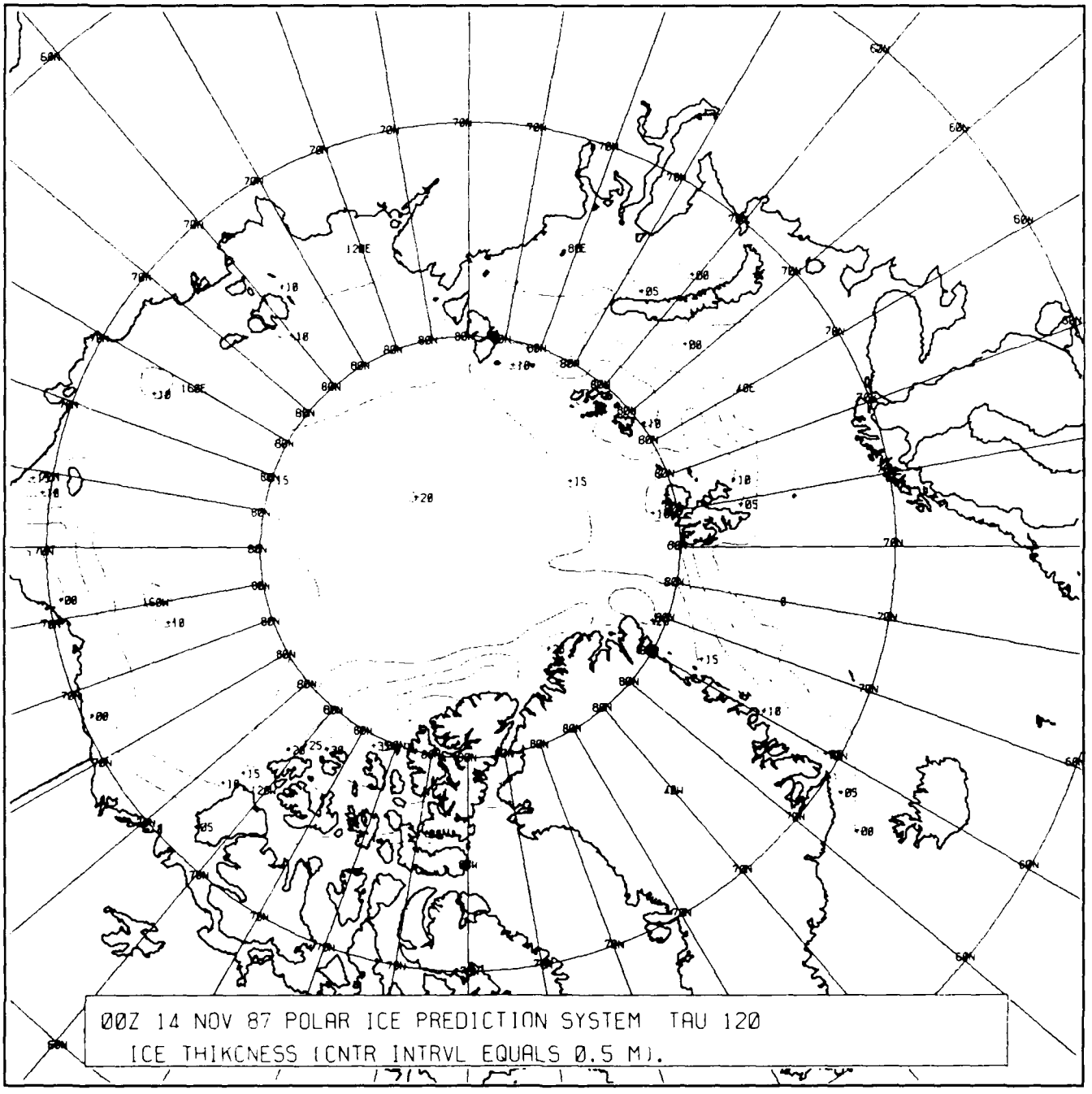

Figure 23b. Tau 120 forecasted ice thickness from the 14 November 1987 run. Contour interval is 0.5 m.

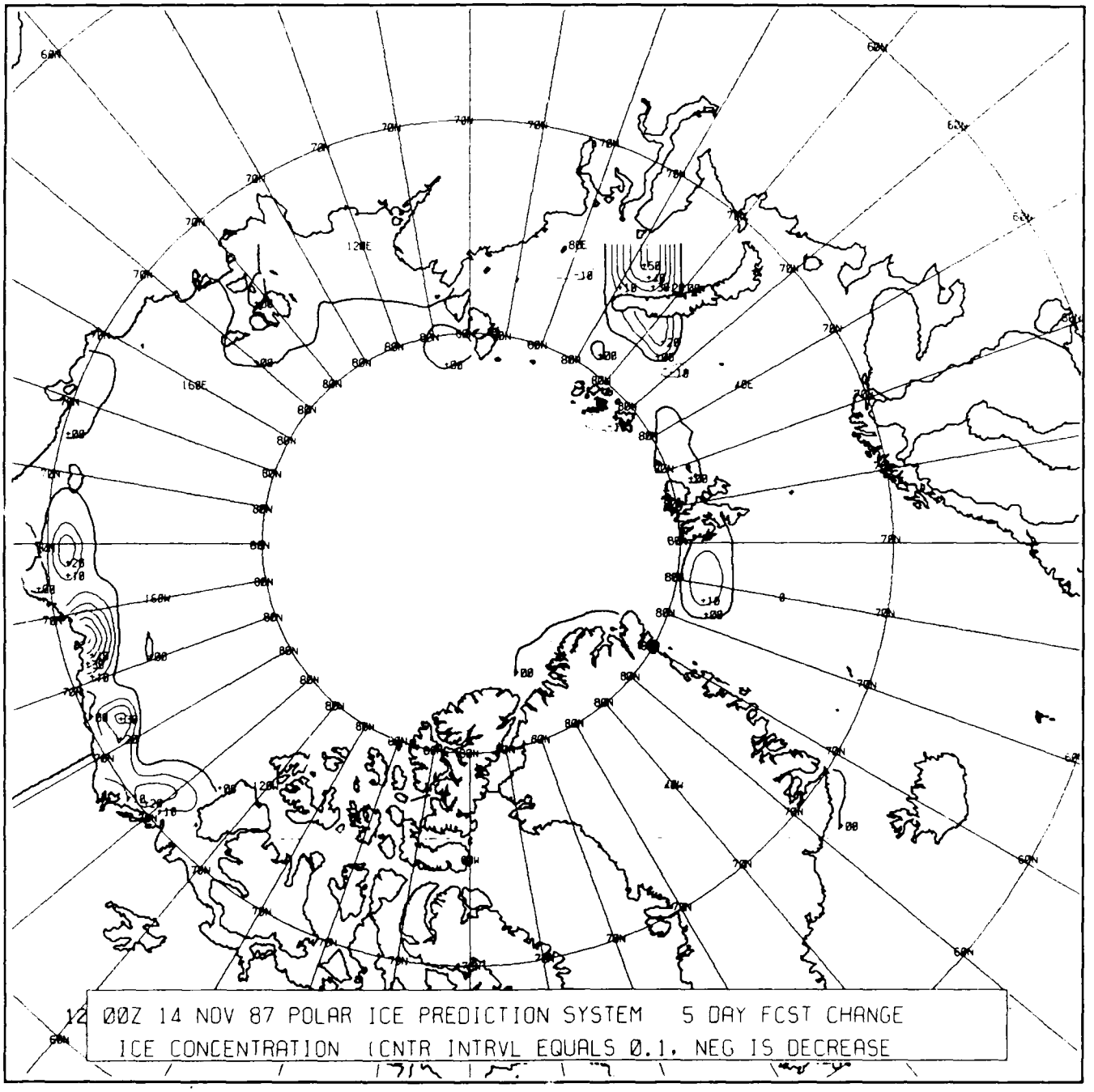

Figure 24a. PIPS 5-day forecasted change in ice concentration. Contour interval is 0.1 or 10%.

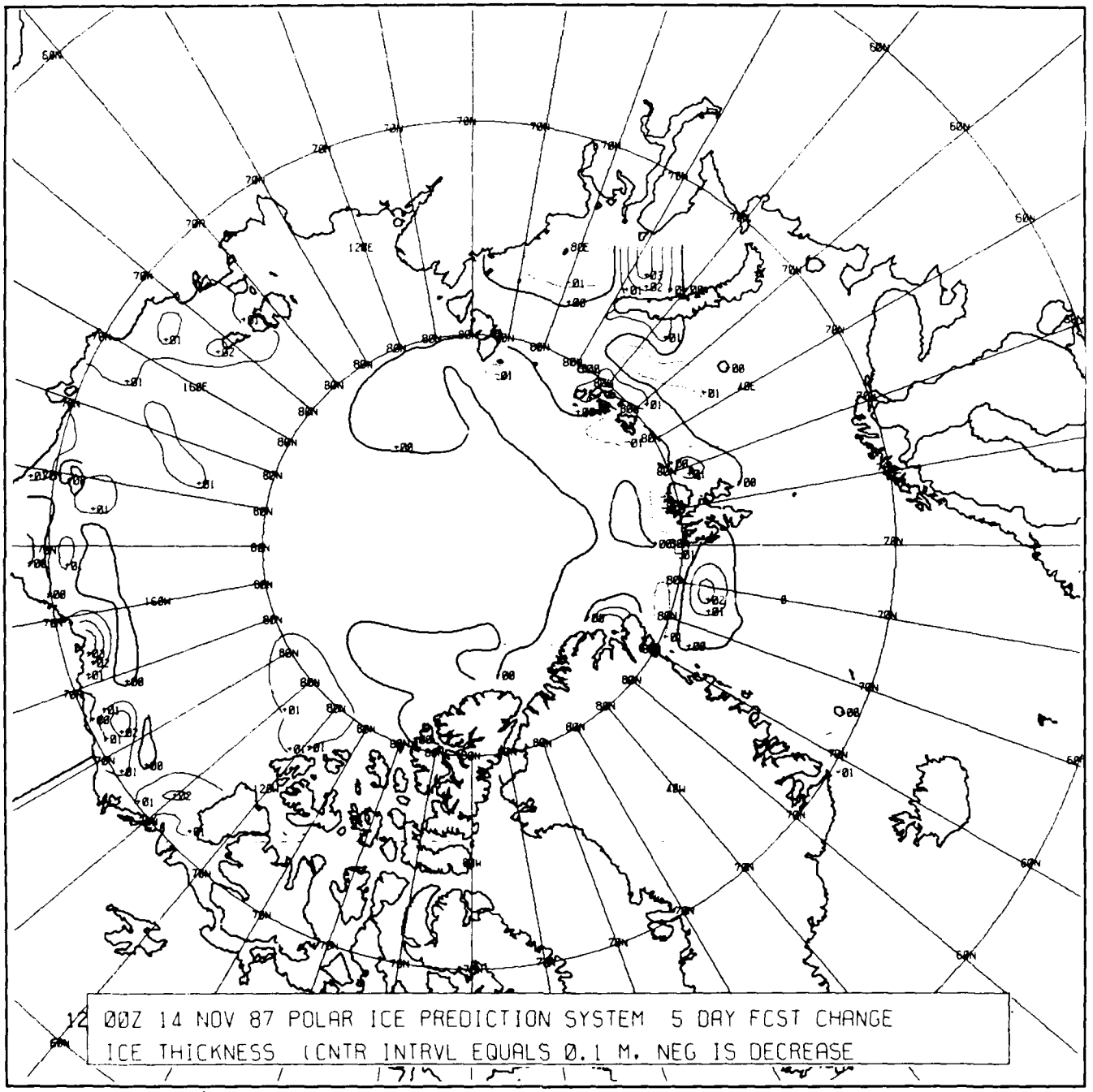

Figure 24b. PIPS 5-day forecasted change in ice thickness. Contour interval is 0.1 m.

Distribution List

Asst Secretary of the Navy
(Research, Engineering & Systems)
Navy Department
Washington DC 20350-1000

Chief of Naval Operations
Navy Department (OP-02)
Washington DC 20350-2000

Chief of Naval Operations
Navy Department (OP-71)
Washington DC 20350-2000

Director
National Ocean Data Center
WSC1 Room 103
6001 Executive Blvd.
Attn: G. W. Withee
Rockville MD 20852

Chief of Naval Operations
Navy Department (OP-987)
Washington DC 20350-2000

Oceanographer of the Navy
Chief of Naval Operations
Attn: OP-096
U.S. Naval Observatory
34th & Mass Ave., NW
Washington DC 20390-1800

Commander
Naval Air Development Center
Warminster PA 18974-5000

Commanding Officer
Naval Coastal Systems Center
Panama City FL 32407-5000

Commander
Space & Naval Warfare Sys Com
Washington DC 20363-5100

Commanding Officer
Naval Environmental Prediction
Research Facility
Monterey CA 93943-5006

Commander
Naval Facilities Eng Command
Naval Facilities Eng Command Headquarters
200 Stovall St.
Alexandria VA 22332-2300

Commanding Officer
Naval Ocean R&D Activity
Attn: Code 100
Stennis Space Center MS 39529-5004

Commanding Officer
Naval Ocean R&D Activity
Attn: Code 125L (13)
Stennis Space Center MS 39529-5004

Commanding Officer
Naval Ocean R&D Activity
Attn: Code 125P (1)
Stennis Space Center MS 39529-5004

Commanding Officer
Naval Ocean R&D Activity
Attn: Code 105
Stennis Space Center MS 39529-5004

Commanding Officer
Naval Ocean R&D Activity
Attn: Code 115
Stennis Space Center MS 39529-5004

Commanding Officer
Naval Ocean R&D Activity
Attn: Code 200
Stennis Space Center MS 39529-5004

Commanding Officer
Naval Ocean R&D Activity
Attn: Code 300
Stennis Space Center MS 39529-5004

Commanding Officer
Naval Research Laboratory
Washington DC 20375

Commander
Naval Oceanography Command
Stennis Space Center MS 39529-5000

Commanding Officer
Fleet Numerical Oceanography Center
Monterey CA 93943-5005

Commanding Officer
Naval Oceanographic Office
Stennis Space Center MS 39522-5001

Commander
Naval Ocean Systems Center
San Diego CA 92152-5000

Commanding Officer
ONR Branch Office
Box 39
FPO New York NY 09510-0700

Commander
David W. Taylor Naval Research Center
Bethesda MD 20084-5000

Commander
Naval Surface Weapons Center
Dahlgren VA 22448-5000

Commanding Officer
Naval Underwater Systems Center
Newport RI 02841-5047

Superintendent
Naval Postgraduate School
Monterey CA 93943

Director of Navy Laboratories
Rm 1062, Crystal Plaza Bldg 5
Department of the Navy
Washington DC 20360

Officer in Charge
New London Laboratory
Naval Underwater Sys Cen Det
New London CT 06320

Director
Office of Naval Research
Attn: Code 10
800 N. Quincy St.
Arlington VA 22217-5000

Director
Woods Hole Oceanographic Inst
P.O. Box 32
Woods Hole MA 02543

University of California
Scripps Institute of Oceanography
P.O. Box 6049
San Diego CA 92106

Officer in Charge
Naval Surface Weapons Center Det
White Oak Laboratory
10901 New Hampshire Ave.
Attn: Library
Silver Spring MD 20903-5000

Commanding Officer
Fleet Anti-Sub Warfare Training Center, Atlantic
Naval Station
Norfolk VA 23511-6495

Brooke Farquhar
NORDA Liaison Office
Crystal Plaza #5, Room 802
2211 Jefferson Davis Hwy.
Arlington VA 22202-5000

Director
Defense Mapping Agency Sys Cen
Attn: SGWN
12100 Sunset Hill Rd. #200
Reston VA 22090-3207

NORDA
Code 125 EX
Stennis Space Center MS 39529-5004
(Unlimited only)

Director
Office of Naval Technology
Attn: Dr. P. Selwyn, Code 20
800 N. Quincy St.
Arlington VA 22217-5000

Director
Office of Naval Technology
Attn: Dr. C. V. Votaw, Code 234
800 N. Quincy St.
Arlington VA 22217-5000

Director
Office of Naval Technology
Attn: Dr. M. Briscoe, Code 228
800 N. Quincy St.
Arlington VA 22217-5000

Director
Office of Naval Research
Attn: Dr. E. Hartwig, Code 112
800 N. Quincy St.
Arlington VA 22217-5000

Director
Office of Naval Research
Attn: Code 12
800 N. Quincy St.
Arlington VA 22217-5000

Director
Office of Naval Research
Attn: Dr. E. Silva, Code 10D/10P
800 N. Quincy St.
Arlington VA 22217-5000

Chief of Naval Operations
Navy Department (OP-0962X)
Attn: Mr. R. Feden
Washington DC 20350-2000

Commander
Naval Sea Systems Command
Naval Sea Systems Command Headquarters
Washington DC 20362-5101

Commanding Officer
Naval Civil Engineering Laboratory
Port Hueneme CA 93043

Commander
Naval Air Systems Command
Naval Air Systems Command Headquarters
Washington DC 20361-0001

Pennsylvania State University
Applied Research Laboratory
P.O. Box 30
State College PA 16801

University of Texas at Austin
Applied Research Laboratories
P.O. Box 8029
Austin TX 78713-8029

Johns Hopkins University
Applied Physics Laboratory
Johns Hopkins Rd.
Laurel MD 20707

University of Washington
Applied Physics Laboratory
1013 Northeast 40th St.
Seattle WA 98105

UNCLASSIFIED

SECURITY CLASSIFICATION OF THIS PAGE

REPORT DOCUMENTATION PAGE

1a. REPORT SECURITY CLASSIFICATION Unclassified	1b. RESTRICTIVE MARKINGS None
2a. SECURITY CLASSIFICATION AUTHORITY	3. DISTRIBUTION/AVAILABILITY OF REPORT Approved for public release; distribution is unlimited. Naval Ocean Research and Development Activity, Stennis Space Center, Mississippi 39529-5004.
2b. DECLASSIFICATION/DOWNGRADING SCHEDULE	
4. PERFORMING ORGANIZATION REPORT NUMBER(S) NORDA Report 212	5. MONITORING ORGANIZATION REPORT NUMBER(S) NORDA Report 212
6. NAME OF PERFORMING ORGANIZATION Naval Ocean Research and Development Activity	7a. NAME OF MONITORING ORGANIZATION Naval Ocean Research and Development Activity
6c. ADDRESS (City, State, and ZIP Code) Ocean Science Directorate Stennis Space Center, Mississippi 39529-5004	7b. ADDRESS (City, State, and ZIP Code) Ocean Science Directorate Stennis Space Center, Mississippi 39529-5004
8a. NAME OF FUNDING/SPONSORING ORGANIZATION U.S. Navy Space and Naval Warfare Systems Command 8b. OFFICE SYMBOL (If applicable)	9. PROCUREMENT INSTRUMENT IDENTIFICATION NUMBER
8c. ADDRESS (City, State, and ZIP Code) Code PDW 106-8 Washington, D.C. 20361	10. SOURCE OF FUNDING NOS PROGRAM ELEMENT NO. 63207N; PROJECT NO 00513; TASK NO. 999; WORK UNIT NO. DN894428
11. TITLE (Include Security Classification) The Polar Ice Prediction System—A Sea Ice Forecasting System	
12. PERSONAL AUTHOR(S) Ruth H. Preller, *Pamela G. Posey	
13a. TYPE OF REPORT Final	13b. TIME COVERED From _____ To _____
14. DATE OF REPORT (Yr., Mo., Day) April 1989	15. PAGE COUNT 45
16. SUPPLEMENTARY NOTATION *Berkeley Research Associates, P.O. Box 852, Springfield, Virginia 22150	
17. COSATI CODES FIELD / GROUP / SUB. GR.	18. SUBJECT TERMS (Continue on reverse if necessary and identify by block number) sea ice forecasting, sea ice models, sea ice analysis

19. ABSTRACT (Continue on reverse if necessary and identify by block number)

The Polar Ice Prediction System (PIPS), based on the Hibler dynamic/thermodynamic sea ice model, was developed as an upgrade to the existing sea ice products available at the U.S. Navy's Fleet Numerical Oceanography Center (FNOC). It was also designed to provide new sea ice products that could be used as guidance by the Naval Polar Oceanography Center (NPOC). The operational testing of PIPS showed that the ice drift from the model was excessive in magnitude when compared to ice drift from Arctic buoys. As a result, the PIPS forcing was changed from planetary boundary layer model winds to geostrophic winds calculated from forecast surface pressures. Resultant PIPS ice drifts were more accurate than those calculated by the existing operational model - the Thorndike and Colony free-drift model. The operational test also indicated a need to reduce the model time step from 24 to 6 hours. Reducing the time step allowed for better resolution of atmospheric heat fluxes and improved the model's capability to predict ice edge location. PIPS results also showed great improvement when updated by an ice concentration analysis for the Arctic derived by NPOC. This updating technique is now an integral part of the PIPS system and takes place approximately once per week.

As a result of this testing and the associated improvements made to the model, PIPS was declared operational on 1 September 1987. Examples of PIPS output and results from model-data comparisons are presented.

20. DISTRIBUTION/AVAILABILITY OF ABSTRACT UNCLASSIFIED/UNLIMITED ☐ SAME AS RPT. ■ DTIC USERS ☐	21. ABSTRACT SECURITY CLASSIFICATION Unclassified	
22a. NAME OF RESPONSIBLE INDIVIDUAL R. H. Preller	22b. TELEPHONE NUMBER (Include Area Code) (601) 688-5444	22c. OFFICE SYMBOL Code 322

DD FORM 1473, 83 APR EDITION OF 1 JAN 73 IS OBSOLETE

UNCLASSIFIED

SECURITY CLASSIFICATION OF THIS PAGE